Molecular Biology of the Cell
Vol. 17, 3156–3175, July 2006

Rab10 Regulates Membrane Transport through Early Endosomes of Polarized Madin-Darby Canine Kidney Cells[V]

Clifford M. Babbey,* Nahid Ahktar,* Exing Wang,* Carlos Chih-Hsiung Chen,† Barth D. Grant,† and Kenneth W. Dunn*

*Department of Medicine, Division of Nephrology, Indiana University Medical Center, Indianapolis, IN 46202; and †Department of Molecular Biology and Biochemistry, Rutgers University, Piscataway, NJ 08854

Submitted August 25, 2005; Revised March 21, 2006; Accepted April 14, 2006
Monitoring Editor: Keith Mostov

Rab10, a protein originally isolated from Madin-Darby Canine Kidney (MDCK) epithelial cells, belongs to a family of Rab proteins that includes Rab8 and Rab13. Although both Rab8 and Rab13 have been found to mediate polarized membrane transport, the function of Rab10 in mammalian cells has not yet been established. We have used quantitative confocal microscopy of polarized MDCK cells expressing GFP chimeras of wild-type and mutant forms of Rab10 to analyze the function of Rab10 in polarized cells. These studies demonstrate that Rab10 is specifically associated with the common endosomes of MDCK cells, accessible to endocytic probes internalized from either the apical or basolateral plasma membrane domains. Expression of mutant Rab10 defective for either GTP hydrolysis or GTP binding increased recycling from early compartments on the basolateral endocytic pathway without affecting recycling from later compartments or the apical recycling pathway. These results suggest that Rab10 mediates transport from basolateral sorting endosomes to common endosomes.

INTRODUCTION

The function of eukaryotic cells depends upon a highly orchestrated system of membrane transport in which proteins and lipids are sorted and specifically transported to particular membrane compartments. In the case of epithelial cells, this includes sorting of proteins to either the apical or basolateral surface of the plasma membrane. The processes by which proteins are sorted into transport vesicles and vesicles are formed, transported, and fused with specific target compartments is mediated by the concerted actions of monomeric Rab proteins, SNARE (soluble *n*-ethyl-maleimide–sensitive factor attachment protein receptor) proteins and their effectors (Rodman and Wandinger-Ness, 2000; Deneka *et al.,* 2003).

Rab10, first isolated from a clone of Madin-Darby Canine kidney (MDCK) cells (Chavrier *et al.,* 1990) belongs to a subfamily of Rab proteins that includes Rab8 and Rab13. This subfamily of Rabs represents the closest mammalian relatives of the Sec4p (Chen *et al.,* 1993; Pereira-Leal and Seabra, 2001), one of the first described Rab proteins, which mediates polarized transport from the *trans*-Golgi network (TGN) to the site of bud formation in yeast (Salminen and Novick, 1987; Walworth *et al.,* 1989). Like Sec4p, Rab8 and Rab13 have also been associated with polarized membrane transport. Rab8 has been found to regulate transport from the TGN to the basolateral membrane of polarized MDCK cells (Huber *et al.,* 1993; Ang *et al.,* 2003), and both Rab8 and Rab13 have been associated with junctional complex dynamics in epithelial cells (Zahraoui *et al.,* 1994; Marzesco *et al.,* 2002; Lau and Mruk, 2003; Kohler *et al.,* 2004; Morimoto *et al.,* 2005).

In previous studies, Rab10 has been morphologically associated with the Golgi complex of fibroblasts (Chen *et al.,* 1993) and sea urchin embryonic cells (Leaf and Blum, 1998). However, in a recent study, Chen *et al.* (2006) demonstrate that Rab10 localizes to both endosomes and the TGN and regulates an early stage of basolateral endocytic recycling in the intestinal epithelia of *Caenorhabditis elegans*. We have characterized the intracellular localization and function of GFP chimeras of wild-type and mutant forms of Rab10 in polarized MDCK cells. These studies demonstrate that Rab10 is closely associated with common endosomes, accessible to both the apical and the basolateral recycling pathways. Expression of mutant Rab10 defective for either GTP hydrolysis or GTP binding increased recycling from early compartments on the basolateral endocytic pathway without affecting recycling from later compartments or affecting recycling of apically internalized IgA. These results suggest that Rab10 mediates transport from basolateral sorting endosomes to common endosomes.

This article was published online ahead of print in *MBC in Press* (http://www.molbiolcell.org/cgi/doi/10.1091/mbc.E05–08–0799) on April 26, 2006.

[V] The online version of this article contains supplemental material at *MBC Online* (http://www.molbiolcell.org).

Address correspondence to: Kenneth W. Dunn (kwdunn@iupui.edu).

Abbreviations used: ARE, apical recycling endosome; MDCK, Madin-Darby canine kidney cells; pIgR, polymeric Ig receptor; Tf, transferrin; TfR, transferrin receptor; TGN, *trans*-Golgi network.

MATERIALS AND METHODS

Cell Culture

Studies were conducted using PTR cells, MDCK strain II cells transfected with both the human transferrin receptor (TfR) and the rabbit polymeric immuno-

globulin (Ig) receptor (pIgR), previously described (Brown *et al.*, 2000; Wang *et al.*, 2000, 2001). Previous studies have demonstrated that the transfected human TfR is expressed on the basolateral membrane of these cells, that Tf and IgA binding are specific and that the kinetics of Tf recycling and pIgR transcytosis agree well with previously published values for the parental cells (Apodaca *et al.*, 1994) and for another MDCK cell line transfected with the human TfR (Odorizzi *et al.*, 1996).

PTR cells were grown in MEM (Invitrogen, Grand Island, NY) with 8% fetal bovine serum, 1% L-glutamine, streptomycin, and 0.05% hygromycin (Calbiochem, San Diego, CA). Cells were passed every 3–4 d and growth medium was changed daily. New cultures of cells were thawed every 4–5 wk. For fluorescence experiments, cells were plated at confluence on the bottoms of collagen-coated Millipore CM 12-mm filters (Millipore, Bedford, MA) and cultured for 4–5 d before experiments, as described previously (Brown *et al.*, 2000; Wang *et al.*, 2000, 2001). Bottom-seeding was accomplished by creating a cup on the underside of the filter units by wrapping parafilm around the base of the filter unit. The filter units were inverted and cells seeded into this parafilm cup overnight. The following morning, the parafilm was removed, the filters were removed to their normal orientation in 24-well dishes, and the cells were then grown hanging from the filter. Previous studies have demonstrated that monolayers grown in this way become impermeable, with transepithelial resistance reaching 450 Ω/cm^2 as measured with a Millipore Millicell ERS resistance meter and with cells developing tight junctions (as assessed by immunofluorescence detection of the tight junction protein ZO-1) and a polarized distribution of TfR.

Plasmids and Transient Transfection

Amino terminal GFP chimeras of rab10 were produced using human rab10 cDNA (UMR cDNA Resource Center; www.cDNA.org), which was PCR amplified with primers containing Gateway recombination sequences attB1 and attB2 and cloned into entry vector pDONR201 per manufacturer's protocol (Invitrogen, Carlsbad, CA). The rab10 cDNA was then transferred into a Gateway destination vector prepared in-house composed of pCDNA3.1 modified with EGFP coding sequences and a Gateway cloning cassette (complete plasmid sequences available upon request). Mutant forms of rab10 were prepared using the Quickchange kit per manufacturer's protocol (Stratagene, La Jolla, CA).

An amino terminal YFP chimera of rab10 was generated by amplifying the rab10 gene with PfuTurbo polymerase (Stratagene), using the plasmid above as a template. The amplification primers introduced a 5′ HindIII site and a 3′ EcoRI site, which were used to clone the amplicon into the pEYFP plasmid (Clontech, Palo Alto, CA). An amino terminal CFP chimera of rab11 was generated by amplifying the rab11 gene with PfuTurbo polymerase (Stratagene), using pEGFP-rab11 as a template. The amplification primers introduced a 5′ BglII site and a 3′ KpnI site, which were used to clone the amplicon into the pECFP plasmid (Clontech).

The plasmid expressing pEGFP-tubulin was obtained from Clontech (BD Biosciences, Mountain View, CA). The pEGFP-rab11 plasmid is as described previously (Wang *et al.*, 2001). All plasmids were verified by DNA sequence analysis.

Cells were transfected immediately after seeding onto filters using GeneJammer transfection agent (Stratagene), per manufacturer's protocol. A ratio of 2.8 μl transfection agent to 0.8 μg plasmid DNA was found to be optimal.

Proteins and Chemicals

Purified dimeric IgA was provided by Prof. J.-P. Vaerman (Catholic University of Louvain, Brussels, Belgium). Human Tf was obtained from Sigma Chemical (St. Louis, MO), and iron was loaded and purified as described in Yamashiro *et al.* (1984). With the exception of Cy3 and Cy5, which was obtained from Amersham (Arlington Heights, IL), all reactive fluorophores were obtained from Molecular Probes (Eugene, OR). BFA was obtained from Epicenter Technologies (Madison, WI). DiI-LDL was obtained from Biomedical Technologies (Stoughton, MA). Anti-furin antibody was obtained from Alexis Biochemicals (Axxora, San Diego, CA), anti-Rab11a antibody was obtained from Zymed (Invitrogen, Carlsbad, CA) and anti-GP-135 was a gift from Robert Bacallao. TxR-conjugated secondary antibodies were obtained from Jackson ImmunoResearch (West Grove, PA). All other reagents were obtained from Sigma Chemical. Fluorescent ligands were prepared as described previously (Brown *et al.*, 2000; Wang *et al.*, 2000, 2001).

Labeling of Cells with Fluorescent Ligands

For fluorescence labelings, cells were incubated at 37°C on a slide warmer in a humidified chamber for 15 min before addition of fluorescent ligands. All incubations were conducted in medium 1 (150 mM NaCl, 20 mM HEPES, 1 mM $CaCl_2$, 5 mM KCl, 1 mM $MgCl_2$, 10 mM glucose, pH 7.4). As described in each study, cells were labeled with 20 μg/ml fluorescent Tf, 60 μg/ml fluorescent IgA, or 10 μg/ml fluorescent LDL. After incubations with fluorescent ligands, filters were rinsed briefly in phosphate-buffered saline (PBS) at 4°C and then fixed with 4% paraformaldehyde in pH 7.4 PBS at 4°C for 15 min. Filters were then rinsed in PBS. The specificity of receptor-mediated uptake of fluorescent IgA and Tf was demonstrated by its inhibition by competition with excess unlabeled ligands. Fluorescent IgA and Tf were both found to efflux the cells with kinetics similar to those of the radiolabeled ligands. Dual-labeling experiments showed the endosomal distributions of ligands conjugated to different fluorophores to be identical.

Microscopy

All experiments were conducted using a Perkin-Elmer Cetus Ultraview confocal microscope system (Norwalk, CT) mounted on a Nikon TE 2000U inverted microscope, using Nikon 60× NA 1.2 water immersion or Nikon 100×, NA 1.4 oil immersion planapochromatic objectives (Melville, NY). The system is equipped with a Hamamatsu Orca-ER CCD system (Bridgewater, NJ). Image volumes were collected by collecting a vertical series of images, each between 0.2 and 0.6 μm apart. Whenever possible signal saturation was avoided, and objects with saturated pixels were omitted from quantifications.

As mentioned previously, cells were grown on the underside of Millipore filter units. After removing the legs of the filter units, living or fixed cells were observed by placing the entire filter unit on two 50-μm tape spacers attached to the coverslip of a coverslip-bottomed 35-mm dish (Mattek, Ashland, MA) mounted on the stage of an inverted microscope. For live cell studies, incubations were conducted in medium 1 on the microscope stage, with basolateral ligands added to the filter cup, whereas apical ligands were added to the well of the coverslip-bottomed dish. Temperature was maintained with a microscope stage heater, using either a Warner Instruments TC324B (Hamden, CT) or Medical Systems Corp. PDMI-2 (Greenvale, NY). Fixed cells were imaged immediately after fixation in PBS containing 2% DABCO (Sigma Chemical).

Immunofluorescence Localizations

For immunolocalizations of furin, Rab11a and gp135, cells were labeled as indicated and then fixed as described above. Cells were then washed three times with 10 mM glycine in PBS, pH 7.4, for 10 min. Cells were then permeablized in 0.025% Saponin for 5 min and nonspecific sites were blocked in 1% BSA + 0.025% Saponin + 0.05% fish skin gelatin in PBS–glycine for 5 min. Cells were incubated with primary antibodies and rinsed three times with PBS followed by the incubation with the TxR-sheep anti-mouse antibody for 1 h at room temperature or with TxR-donkey anti-sheep at room temperature for 1 more hour.

Image Processing for Presentation

Image processing was conducted using Metamorph software (Universal Imaging, West Chester, PA). For images with poor signal-to-noise, images were subsequently averaged spatially using a 3 × 3 low pass filter. Images shown in figures were contrast stretched to enhance the visibility of dim structures, and specific care was taken never to enhance the contrast in such a way that dim objects were deleted from an image. Images to be compared were always contrast enhanced identically. Montages were assembled and annotated using Photoshop (Adobe, Mountain View, CA). Volume renderings were conducted using Voxx, a PC-based image analysis program developed at the Indiana Center for Biological Microscopy (Clendenon *et al.*, 2002) and available at no charge (http://nephrology.iupui.edu/imaging/voxx).

Cross-correlation Analysis

Cross-correlation image analysis was conducted as described previously (Brown *et al.*, 2000; Wang *et al.*, 2001). Three-dimensional (3D) image volumes of each probe were collected. A maximum projection of each volume was constructed, and Pearson's r between the two images was calculated for a 32-pixel-diameter circular region (corresponding to a 6-μm diameter in the sample) centered over the projected image of the cell. Maximum correlation values were calculated from samples labeled with two colors of Tf (mean r = 0.96), and random values were calculated from these same images in which one region was rotated 90° relative to the other (mean r = 0.03).

Quantification of Rates of Transferrin Recycling

Previous studies have demonstrated that the recycling of transferrin consists of two pathways, a "fast" pathway from an early compartment and a "slow" pathway from the later recycling compartment (Presley *et al.*, 1993; Sheff *et al.*, 1999; Hao and Maxfield, 2000). To evaluate the role of Rab10 in the slow recycling pathway, cells expressing different forms of GFP-Rab10 were incubated with equimolar ratios of basolateral TxR-Tf and Cy5-Tf for 25 min, then in Cy5-Tf alone for an additional 10 min, and then fixed in 4% PFA. For each image volume, each image plane was background corrected by subtracting the median intensity of a 32 × 32 pixel region surrounding each pixel, and then all of the images of the volume were added together. A region-of-interest was drawn around individual transfected or untransfected cells, and the total pixel intensity for each cell was recorded for each probe.

Recycling was quantified as the fraction of the total recycling pool of receptors, as described below. One filter was fixed immediately after the labeling period, and the ratio of the fluorescence of the two different probes was calculated. This ratio was used as a conversion factor to standardize the fluorescence of the two probes into common units. Thus at the beginning of the chase, the ratio of the fluorescence of the two probes was set to 1 via the conversion factor. This factor was then applied to the measurements of cells

imaged at the end of the chase period to calculate the total standardized fluorescence for each cell. The fraction of total standardized fluorescence resulting from TxR was then measured, and the recycling rate of each cell was quantified from the departure of this ratio from 50%, the standardized ratio measured for cells imaged before the chase.

To evaluate the role of Rab10 in the fast recycling pathway, cells were incubated with TxR-Tf for 20 min at 37°C, rinsed in ice-cold medium 1 for 10 min, incubated with Cy5-Tf for 2 min at 37°C, rinsed in ice-cold medium 1 for 10 min, incubated with TxR-Tf for 4 min at 37°C, and then fixed in 4% PFA. Image volumes were collected and analyzed as described above. Recycling was quantified from the ratio of Cy5-to-TxR fluorescence, a quantity that corrects for variation in expression of TfR between cells. Because a significant amount of the Cy5-Tf is still on the internalization pathway during the 4-min chase interval, it is not feasible to measure the "starting" Cy5/TxR ratio before recycling. Thus we have quantified recycling relative to that observed at 22°, because recycling is disproportionately inhibited relative to internalization at room temperature (Salzman and Maxfield, 1988; Le *et al.*, 1999; Baravelle *et al.*, 2005).

Quantification of Transferrin Internalization Rates

Cells were incubated for 30 min with Cy3-Tf and then with an equimolar ratio of both Cy3-Tf and Cy5-Tf for an additional 4 min and then fixed in 4% PFA. 3D image volumes were collected and analyzed as described above. The amount of fluorescence detected per mole of each probe was standardized using a factor measured from cells labeled with an equimolar mixture of the two probes, imaged after 30 min of uptake with settings identical to those used for the internalization assay. The rate of Tf uptake was quantified as the fraction of total steady state cell-associated Tf fluorescence resulting from the Cy5-Tf internalized during the pulse period.

Quantification of Rates of Apical IgA Recycling

Unlike TfR, which efficiently recycles, pIgR is both recycled and cleaved from the apical plasma membrane. Thus, unlike TfR, the concept of labeling the cellular pool of recycling pIgR to steady state is not justified. For this reason, IgA recycling studies were designed such that the same cells could be evaluated at the beginning and end of a chase period. Cells were incubated for 30 min with Cy5-IgA in the apical chamber, rinsed, and placed in medium 1, with 100 μg/ml trypsin included in the apical and basolateral media. Multiple fields were then immediately imaged using a computerized microscope stage, and the same fields were imaged again after 12 min of incubation. Analyses of fields collected in rapid succession demonstrated that image collection reduced fluorescence by only 1%, indicating that photobleaching minimally affected quantifications. Image volumes were analyzed as described above, except that background correction was accomplished by subtraction of a local background measured manually. The total cell-associated Cy5 fluorescence was then measured at the initial and final time points, and recycling for each cell was quantified from the fraction of the original fluorescence lost before collection of the final volume. In control studies, apical trypsin was found to rapidly cleave apically exposed pIgR-IgA complexes without affecting cell viability or adhesion, consistent with previous studies (Apodaca *et al.*, 1994; Brown *et al.*, 2000)

Quantification of Rates of Efflux of Basolaterally Internalized IgA

Studies were conducted and analyzed as described above, except that cells were incubated with Cy5-IgA in the basolateral chamber for 20 min, and image volumes were collected at both the beginning of the chase and after 20 min in medium 1.

RESULTS

To investigate the role of Rab10 in polarized MDCK cells, we evaluated polarized MDCK cells expressing amino-terminal chimeras of GFP and wild-type or mutant Rab10. In studies of yeast, a similar chimera of GFP and the highly homologous yeast Sec4p protein was targeted and trafficked like endogenous Sec4p and was capable of rescuing the growth defect in cells expressing defective Sec4p (Schott *et al.*, 2002). For this purpose we developed a method for transiently expressing plasmids encoding GFP chimeras of wild-type and mutant Rab proteins in filter-grown cells (see *Materials and Methods*). Using this technique, relatively high frequencies of expression of transfected proteins are obtained (10–20%) in fully polarized cells.

To compare the distribution of Rab10 with well-characterized markers of intracellular trafficking, studies were conducted in the PTR line of MDCK cells, because this cell line is transfected with both the human TfR and the rabbit pIgR. As described in our previous work (Brown *et al.*, 2000; Wang *et al.*, 2000, 2001), the polarity and intracellular kinetics of these receptors is similar to that reported in other MDCK cell lines and these transfected receptors permit sensitive labeling of both the basolateral and apical endocytic pathways. The transfected TfR is polarized to the basolateral membrane, allowing the use of fluorescently labeled Tf as a probe of the basolateral recycling pathway. Although newly synthesized pIgR is directed to the basolateral membrane of transfected MDCK cells, from which it mediates apical transcytosis, a significant fraction of pIgR is expressed at the apical plasma membrane, from which it is internalized and recycled with greater than 95% fidelity (Breitfeld *et al.*, 1989; Leung *et al.*, 1999; Rojas *et al.*, 2001). Thus, the pIgR ligand IgA can be used as a sensitive probe of both the basolateral-to-apical transcytotic pathway and the apical recycling pathway (Apodaca *et al.*, 1994; Brown *et al.*, 2000; Wang *et al.*, 2000, 2001).

GFP-Rab10 Associates with Endosomes in Polarized MDCK Cells, But Not with the **trans-***Golgi Network*

In polarized MDCK cells, GFP-Rab10 is found in vesicular compartments throughout the cell. In contrast to previous studies (Chen *et al.*, 1993; Leaf and Blum, 1998), we find that these vesicular compartments do not correspond to the *trans*-Golgi network (TGN). 3D image volumes collected of MDCK cells expressing GFP-Rab10 and processed for furin immunofluorescence show that GFP-Rab10, the vesicular distribution of GFP-Rab10 is clearly distinct from peri-nuclear tubular distribution of furin in the TGN (Figure 1, A and B). Similar results were obtained using an antibody against gamma-adaptin, another protein enriched in the TGN (our unpublished data).

To determine whether the vesicular structures associated with Rab10 are endosomes, GFP-Rab10–expressing cells were incubated with fluorescent Tf on the basal side of the monolayer. Figure 1, C and D, shows *XY* and *XZ* projections of an image volume of GFP-Rab10 in a cell incubated with fluorescent Tf. Comparison of the GFP and Tf images shows that the vast majority of the vesicles associated with GFP-Rab10 contain internalized Tf (arrows in the figures indicate a few examples). Although these figures demonstrate that GFP-Rab10 colocalizes closely with internalized Tf but not with furin, the relative distributions of these three probes can be better appreciated in the 3D renderings of the image volumes presented in Video 1. (Please note that videos will play more smoothly if downloaded and played rather than played directly through the browser.)

Similar results were found over a range of levels of expression of GFP-Rab10. Figure 1, E and F, shows *XY* and *XZ* projections of a field containing cells expressing a fourfold range of GFP-Rab10. In both the low- and high-expressing cells, GFP-Rab10 predominantly associates with Tf-containing endosomes. Furthermore, comparison with nontransfected cells shows that the morphology of endosomes containing Tf appears unaltered in cells expressing GFP-Rab10. Although the cells shown in this figure are fixed, identical results were obtained in cells imaged while living (our unpublished data).

GFP-Rab10 Associates with Common Endosomes, at the Junction of Apical and Basolateral Recycling Pathways

Tf has been associated with a variety of different endocytic compartments in polarized epithelial cells, variously referred to as basolateral sorting endosomes, basolateral recycling endosomes, common endosomes, and the subapical

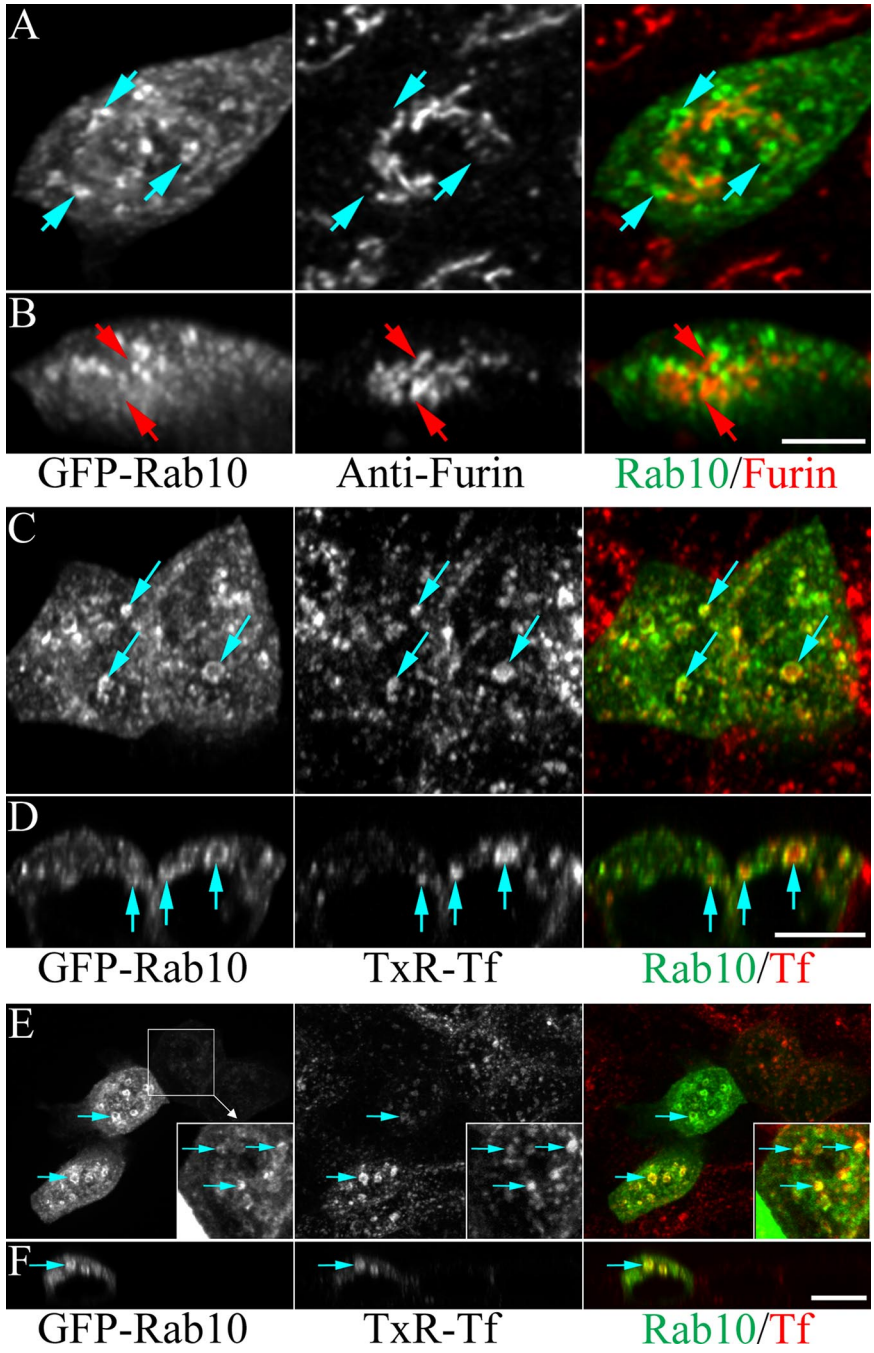

Figure 1. GFP-Rab10 associates with endosomes and not with the TGN of polarized MDCK cells. (A and B) Cells expressing GFP-Rab10 were processed for immunofluorescence using an anti-furin antibody. Three-dimensional image volumes were collected, one of which is presented as a single projection of the collected images (*XY* projection, A) or as an *XZ* projection of a subset of vertical sections through the cells (B). The projections are combined into a single color image in the third column, with GFP shown in green and furin immunofluorescence shown in red. Blue arrows indicate GFP-Rab10 associated with vesicular compartments lacking furin immunofluorescence, whereas red arrows in the *XZ* projection indicate furin compartments lacking GFP-Rab10. (C and D) Cells expressing GFP-Rab10 were incubated in basolateral TxR-Tf for 20 min before fixation and 3D imaging. A close correspondence between the two can be seen in both the *XY* and *XZ* projections (C and D, respectively). Arrows indicate a few examples of GFP-Rab10 (green) associated with compartments containing internalized TxR-Tf (red). Volume renderings of the cells shown in these figures are shown in Video 1. (E and F) *XY* and *XZ* projections of a field of cells similar to those in C, but expressing different levels of GFP-Rab10, showing that the association of GFP-Rab10 with Tf-containing endosomes is independent of the level of GFP-Rab10 expression over a fourfold range. The inset is a 2× magnification whose contrast has been enhanced to display the weak GFP fluorescence. Scale bars, 5 μm (A and B) or 10 μm (C–F).

compartment (e.g., Apodaca *et al.*, 1994; Odorizzi *et al.*, 1996; Futter *et al.*, 1998; Sheff *et al.*, 1999; Brown *et al.*, 2000; Wang *et al.*, 2000, 2001; Hoekstra *et al.*, 2004). Although some of this variety reflects nomenclature and/or experimental differences, the basolateral recycling pathway followed by Tf clearly includes functionally distinct compartments (Sheff *et al.*, 1999; Brown *et al.*, 2000). To better understand the function of Rab10, further studies were conducted to identify the nature of the endosomes with which it associates.

Our previous studies have demonstrated that Tf is initially internalized into basolateral sorting endosomes, along with ligands such as LDL and IgA (Brown *et al.*, 2000). Subsequently, Tf is directed to common endosomes from which it is recycled to the basolateral plasma membrane (Wang *et al.*, 2000). Two sets of studies were conducted to address the question of whether Rab10 associates with sorting endosomes. In the first, cells were incubated for 2 min with basolateral Tf, a period in which internalized Tf is restricted to the earliest endosomes, located immediately adjacent to the lateral membrane. In the cells shown in Figure 2, Tf is found in lateral compartments in the apical (A) and basal portions of the cells (B). GFP-Rab10 is associated with relatively few of these compartments; the majority of GFP-Rab10 is associated with apical compartments away from the lateral membrane.

These results demonstrate that little Rab10 appears to be associated with the earliest basolateral endosomes. In previous studies of polarized MDCK cells, we have demon-

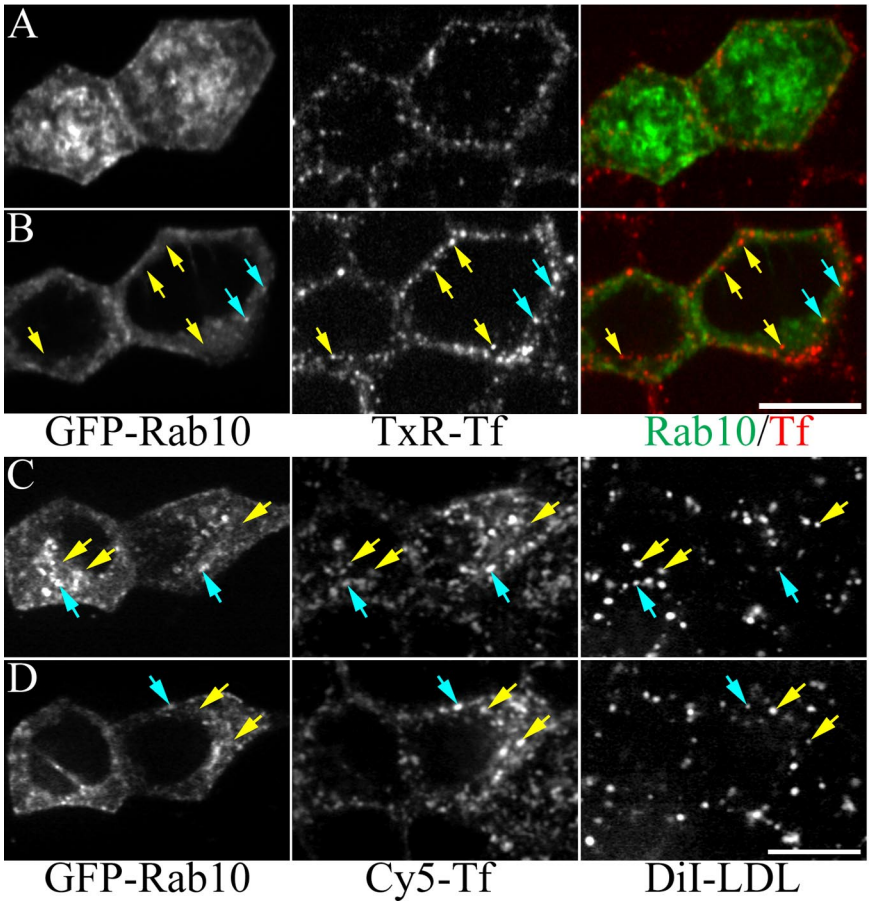

Figure 2. GFP-Rab10 associates with a small fraction of basolateral sorting endosomes. Cells expressing GFP-Rab10 were incubated in basolateral TxR-Tf for 2 min and fixed and 3D image volumes were collected. (A) An optical section collected from the apical region of the cells. (B) An optical section collected ~4 μm lower in the cells. Although GFP-Rab10 (green) is associated with punctate structures, it is largely absent from the sharply punctate lateral compartments containing internalized TxR-Tf (red). Yellow arrows indicate lateral compartments containing Tf but not Rab10, and blue arrows indicate compartments containing both. (C and D) Cells expressing GFP-Rab10 were incubated with dil-LDL and Cy5-Tf for 20 min and fixed, and 3D image volumes were collected. Projections of a 2-μm-thick region and a 4-μm-thick region lower in the cells are shown in C and D, respectively. Arrows indicate sorting endosomes, containing both Tf and LDL, and blue arrows indicate sorting endosomes also associated with GFP-Rab10. Scale bar, 10 μm.

strated that Tf and LDL are both internalized into the same compartments, from which Tf is rapidly sorted (Brown *et al.*, 2000). In this and previous work in fibroblasts (Dunn *et al.*, 1989; Dunn and Maxfield, 1992), we have identified these compartments as sorting endosomes. To determine whether Rab10 could be detected in sorting endosomes, as defined by the combined presence of internalized Tf and LDL, image volumes were collected of Rab10-expressing cells incubated with fluorescent LDL and Tf. The results of these studies are shown in Figure 2, C and D. As in previous figures, the distribution of Rab10 closely matches that of internalized Tf. Close inspection also shows the presence of sorting endosomes, containing both Tf and LDL (indicated with arrows). Consistent with the studies shown in Figure 2, A and B, relatively few of these sorting endosomes are also associated with Rab10 (indicated with blue arrows).

Taken together, our studies suggest that Rab10 is predominantly associated with a downstream recycling compartment. In previous studies, we have demonstrated that this downstream recycling compartment consists of common endosomes that are accessible to apically internalized ligands (Brown *et al.*, 2000; Wang *et al.*, 2000). To address the question of whether Rab10 compartments are accessible to the apical endocytic pathway, cells were incubated for 20 min with fluorescent Tf on the basal side and fluorescent IgA on the apical side of the monolayer. The *XY* and *XZ* projections of the image volumes collected of these cells (Figure 3, A and B) show that the Tf-containing compartments with which GFP-Rab10 associates are accessible to apically internalized IgA, thus identifying them as common endosomes.

Previous studies have demonstrated that apical sorting endosomes, the first compartment on the apical endocytic pathway, are minimally accessible to basolaterally internalized Tf (Leung *et al.*, 2000). Therefore, the close association of Rab10 with Tf-containing endosomes suggests that Rab10 is not associated with apical sorting endosomes. The question of whether Rab10 can be found associated with apical sorting endosomes was addressed by incubating cells for 14 min with basolateral TxR-Tf, with Cy5-IgA added to the medium on the apical side of the cells for the final 4 min of the incubation. At this point, the majority of internalized IgA is found in punctate vesicles at the very apex of the cells (yellow arrows in Figure 3C) with relatively little IgA present in lower focal planes (Figure 3D). GFP-Rab10 is not associated with these punctate, apical compartments but, similar to previous figures, is closely associated with medial compartments containing basolaterally internalized Tf. The absence of GFP-Rab10 from the apical IgA-containing endosomes is especially obvious in the projected *XZ* images shown in Figure 3E. Similar to previous studies (Wang *et al.*, 2000), even after incubations of only 4 min, a fraction of apically internalized IgA accesses Tf-containing common endosomes which, consistent with the previous figure, are associated with Rab10 (blue arrows in Figure 3, D and E).

In Figure 3E, we have outlined the apical extent of the cells, as determined separately from the diffuse cytosolic GFP fluorescence. It is clear in these images that the punctate IgA fluorescence arises from within the cells, rather than from surface-bound IgA aggregates. To ensure that surface-bound IgA does not confuse identification of apical early

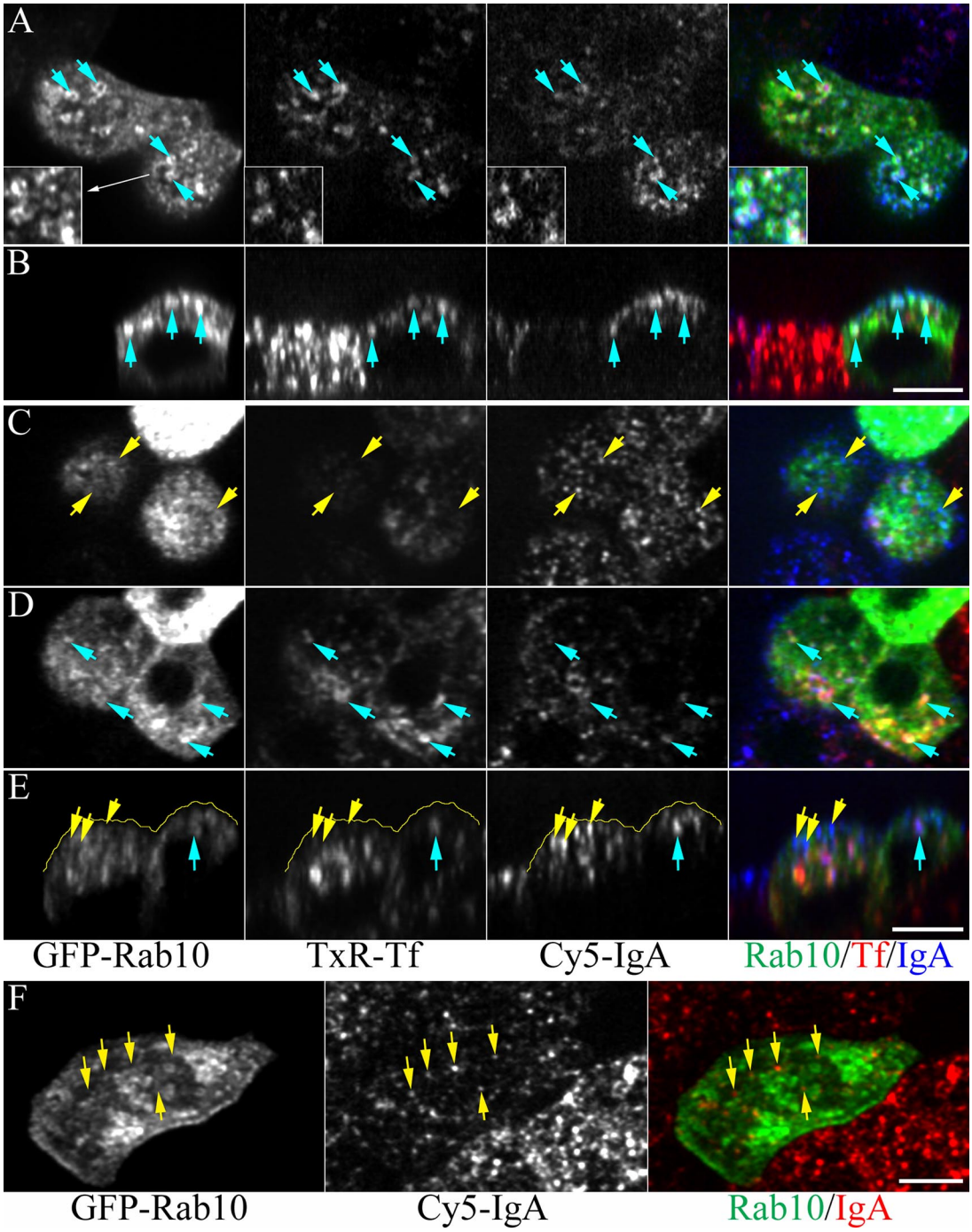

Figure 3. GFP-Rab10 associates with common endosomes accessible to apically internalized IgA. (A and B) Cells expressing GFP-Rab10 (green) were incubated with basal TxR-Tf and apical Cy5-IgA for 20 min. A projection of three subapical focal planes is presented in A, and a projection of vertical sections from the lower part of the field is presented in B. A large fraction of the Tf-containing endosomes with which GFP-Rab10 associates also contain apically internalized IgA, of few of which are indicated with blue arrows. (C–E) Cells expressing GFP-Rab10 (green) were incubated for 14 min with TxR-Tf on the basal side, with Cy5-IgA present on the apical side of the monolayer for the final 4 min. Projections of images collected at the top (A) and middle (B) regions of the cells show that apically internalized IgA is largely found in sharply punctate compartments at the apex of the cells. These compartments, some of which are indicated with yellow arrows, lack GFP-Rab10 and TxR-Tf, an observation that is especially apparent in the *XZ* sections of two cells presented in C. Blue arrows indicate GFP-Rab10 associated with Tf-containing endosomes. (F) Cells expressing GFP-Rab10 (green) were incubated with Cy5-IgA (red) on the apical side of the monolayer for 4 min, incubated with 100 μg/ml trypsin at 4°, and then fixed. As in the previous figures, apically internalized IgA is largely distributed in sharply punctate endosomes that lack GFP-Rab10 (some of which are indicated with arrows). Scale bars, 10 μm.

endosomes, studies were conducted in which cells were incubated for 4 min with apical IgA and then treated with 100 μg/ml trypsin at 4° before fixation, a treatment determined to efficiently strip surface-bound IgA. The results of

these studies, shown in Figure 3F, are identical to those shown in the previous figures. IgA is largely restricted to sharply punctate apical endosomes that lack detectible Rab10.

Taken together, our data indicate that Rab10 is not detectibly associated with apical sorting endosomes and is associated with only a fraction of basolateral sorting endosomes. The majority of Rab10 associates with common endosomes.

Unlike Rab11a, GFP-Rab10 Is Not Enriched in the Apical Recycling Endosome

The apical recycling endosome (ARE) is an endocytic recycling compartment that consists of vesicular and tubular compartments that are condensed around the microtubule organizing center just below the apical plasma membrane (Apodaca *et al.*, 1994; Brown *et al.*, 2000; Leung *et al.*, 2000; Hoekstra *et al.*, 2004). The ARE is a distinct compartment in MDCK cells that appears to function specifically in the apical recycling pathway; the ARE is depleted of basolaterally recycling Tf, but enriched in internalized IgA, which accumulates in the ARE before transcytotic delivery or recycling to the apical plasma membrane (Apodaca *et al.*, 1994; Brown *et al.*, 2000; Leung *et al.*, 2000; Wang *et al.*, 2000). The ARE is also strongly associated with Rab11a, which regulates apical membrane traffic (Casanova *et al.*, 1999; Brown *et al.*, 2000; Leung *et al.*, 2000). To determine whether Rab10 associates with the ARE, studies were conducted in which the distribution of GFP-Rab10 was compared with that of basolaterally internalized IgA and Rab11a.

Figure 4, A and B, shows *XY* and *XZ* projections of cells incubated with basolateral Tf and IgA for 20 min and then fixed. As in previous figures, comparison of the distribution of GFP-Rab10 and Tf shows a close correspondence between the two. Although some of these compartments also contain internalized IgA (blue arrows, especially in the *XZ* image projection), IgA is largely associated with the ARE, the collection of compartments located at the tops of the cells (indicated with yellow circles in A and yellow arrows in B). Close inspection of the ARE, particularly in the high-magnification inset, shows that although the distributions of GFP-Rab10 and Tf are very similar, they are both absent from the ARE, as labeled with internalized IgA.

The difference between the distributions of GFP-Rab10 and IgA in the ARE is more apparent when compared with the close correspondence in the distributions of IgA and Rab11a, an ARE-associated protein. Figure 4, C and D, shows *XY* and *XZ* projections of a field of cells expressing GFP-Rab11a that were incubated with fluorescent IgA and Tf. In contrast to the images shown above, these cells show a striking colocalization of GFP-Rab11a with internalized IgA, especially in the ARE (indicated with yellow circles in C and yellow arrows in D). As in the previous figure, little or no Tf is detected in the ARE, as labeled with GFP-Rab11a.

A direct comparison between Rab10 and Rab11a is shown in Figure 4, E and F, in which GFP-Rab10–expressing cells were incubated with fluorescent Tf and then processed for Rab11a immunofluorescence. These studies likewise demonstrate that the preponderance of immunolocalized Rab11a associates with the ARE, which lacks both GFP-Rab10 and Tf, whereas GFP-Rab10 closely colocalizes with Tf.

These studies indicate that Rab10, unlike Rab11a, does not associate with the ARE. However, the distributions of multiple probes are difficult to resolve visually, particularly because the morphology of the ARE is variable. To quantify the relationship between the distributions of Rab10, Rab11a, Tf, and IgA, an image cross-correlation analysis was conducted. For this analysis, a projection of the image volume of the cells was produced for a circular region corresponding the position of the ARE. A Pearson's *r* was then calculated, comparing the intensities of the two fluorescent probes at each pixel in the region. Consistent with our visual analysis, we find that the correlation between internalized IgA and GFP-Rab10 is approximately half that between IgA and GFP-Rab11a (Figure 5A). Corresponding results are found in the quantitative comparison of the distributions of GFP-Rab10 and GFP-Rab11a with internalized Tf; whereas the distribution of internalized Tf is highly correlated with GFP-Rab10, it is negatively associated with the distribution of GFP-Rab11a in the region of the ARE, consistent with its exclusion from the ARE (Figure 5B).

The validity of this correlation analysis is demonstrated in Figure 5C. When cells are labeled with Tf conjugated to two different fluors, the two probes are expected to codistribute almost perfectly. In fact we measure a mean correlation of 0.96 between the projected images of two different colors of internalized Tf. Random colocalization was modeled by comparing the two images after rotating one by 90°. Analysis of such image pairs reduced the mean correlation to 0.03.

Mutations in the GTP-binding and GTP-Hydrolysis Domains Alter the Localization of Rab10

The function of Rab proteins depends upon a cycle of GTP binding and hydrolysis, with the GTP-bound form typically considered "active" and the GDP-bound form considered "inactive." To further evaluate the potential functions of Rab10, plasmids encoding canonical site-directed mutant forms of Rab10 were created. One mutant encoded the change of a critical threonine in the GTP-binding domain into an asparagine, creating the T23N mutant. The corresponding mutations in Ras, Rab7, Rab8, Rab11a, and Rab25 have been shown to decrease the affinity of the protein for GTP, resulting in the accumulation of a GDP-bound form (Feig and Cooper, 1988; Peranen *et al.*, 1996; Bucci *et al.*, 2000; Wang *et al.*, 2000). This mutation frequently results in a protein with dominant-negative effects on Rab function; overexpression has been found to alter the function of Rab8 (Moritz *et al.*, 2001) and yeast Sec4p (Walworth *et al.*, 1989), as well as Rab4 (McCaffrey *et al.*, 2001), Rab5 (Stenmark *et al.*, 1994), Rab7 (Feng *et al.*, 1995; Bucci *et al.*, 2000), Rab11 (Ullrich *et al.*, 1996; Wang *et al.*, 2000a), Rab14 (Jununtula *et al.*, 2004), and Rab15 (Zuk and Elferink, 2000). A second mutant was also created, encoding a change from glutamine into leucine at position 68 (Q68L). The corresponding mutation has been found to impair GTP hydrolysis in Ras, Sec4p, Rab11a, and Rab25, thus increasing the amount of GTP-bound form of the protein (Walworth *et al.*, 1992; Frech *et al.*, 1994; Wang *et al.*, 2000). This mutation has been found to have dominant-active effects on the function of a variety of GTPases, with overexpression altering the function of Rab5 (Stenmark *et al.*, 1994), Rab7 (Bucci *et al.*, 2000), Rab8 (Ang *et al.*, 2003), Rab14 (Jununtula *et al.*, 2004), Rab15 (Zuk and Elferink, 1999), and Rab17 (Zacchi *et al.*, 1994).

In contrast to the wild-type protein, GFP-Rab10-T23N was found distributed in the cytosol as well as to intracellular compartments that are not accessible to internalized Tf. Figure 6A shows two such cells, in which the tubular distribution of GFP-Rab10-T23N is distinct from that of internalized Tf. Comparison of these cells with their neighbors shows that expression of the T23N mutant Rab10 has no obvious effect on endosome morphology, nor on the amount of Tf taken up by the cells.

Because the tubular morphology of the compartments associated with GFP-Rab10-T23N resembled that of the TGN, the distribution of the GFP-Rab10-T23N was com-

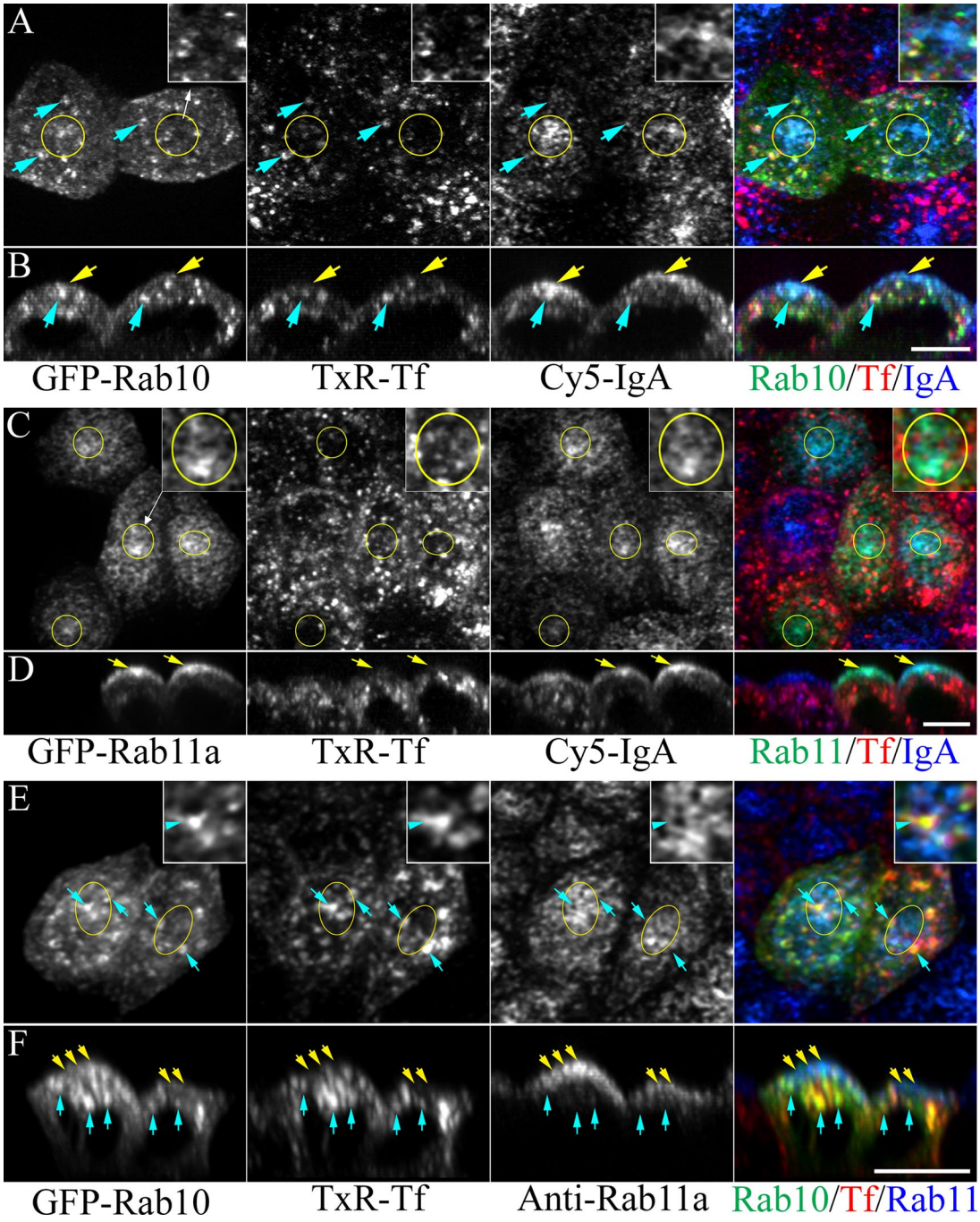

Figure 4. GFP-Rab10 is not associated with the ARE. (A and B) Cells expressing GFP-Rab10 were incubated with TxR-Tf and Cy5-IgA in the basolateral medium for 20 min and fixed. As in previous figures, GFP-Rab10 associates with endosomes containing TxR-Tf, some of which are indicated with blue arrows. However, the preponderance of the Cy5-IgA fluorescence is concentrated in the ARE, which lacks both GFP-Rab10 and TxR-Tf, indicated with yellow circles in the *XY* projections (A) and with yellow arrows in the *XZ* projections (B). The 2× magnification of the ARE region of one of the cells clearly shows that Cy5-IgA accumulated in compartments lacking GFP-Rab10 and TxR-Tf. (C and D). Cells were labeled as in A and B, except that they were transfected with GFP-Rab11a, which has been shown to closely associate with the ARE. In this case, a close correspondence is found between the distribution of GFP-Rab11a and Cy5-IgA, particularly in the regions of the ARE, as indicated with yellow circles in the *XY* projections (C) and yellow arrows in the *XZ* projections (D). As in the previous figure, TxR-Tf is absent from these compartments. The different distribution of TxR-Tf compared with GFP-Rab11a and Cy5-IgA in the ARE of one of the cells is emphasized in the 2× inset in C. (E and F) The distributions of GFP-Rab10 and Rab11a were compared by transfecting cells with GFP-Rab10, incubating them with TxR-Tf, and then processing them for Rab11a immunofluorescence. The colocalization of GFP-Rab10 and TxR-Tf in common endosomes, and their absence from Rab11a-associated AREs is shown in *XY* projections (E) and *XZ* projections (F). The inset in E shows a 2× magnification of one of the cells. Scale bars, 10 μm.

pared with that of immunofluorescently labeled furin. Figure 6B shows that the tubular compartments with which GFP-Rab10-T23N associates contains furin, indicating an association with the TGN.

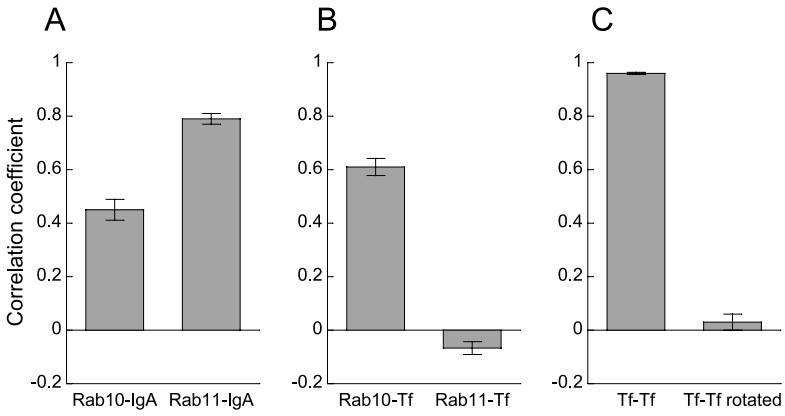

Figure 5. Image cross-correlation analysis of the distributions of GFP-Rab10 and GFP-Rab11a relative to basolaterally internalized Tf and IgA. (A) Correlation analysis comparing the distribution of Cy5-IgA with either GFP-Rab10 or GFP-Rab11a in the ARE region from projected 3D image volumes collected of transfected cells labeled for 20 min with Cy5-IgA. The distribution of Cy5-IgA is much more highly correlated with the ARE-associated GFP-Rab11a ($r = 0.79$, n = 31) than with GFP-Rab10 ($r = 0.45$, n = 22). (B) The opposite relationship is found for internalized TxR-Tf, which is more highly associated with GFP-Rab10 ($r = 0.61$, n = 22), than with GFP-Rab11a ($r = -0.067$, n = 20). (C) The validity of the correlation analysis was verified in samples labeled for 20 min with TxR-Tf and Cy5-Tf, which provide a sample with nearly perfect colocalization. In this case the correlation between TxR-Tf and Cy5-Tf averaged 0.96 (n = 20). Random correlation was modeled by rotating the image of Cy5-Tf 90° before comparison with its partner. In this case, the correlation between the two images averaged 0.03 (n = 20). Differences in all three comparisons were statistically significant, with $p \ll 0.0001$. Data are presented as means ± SEM.

Cells expressing GFP-Rab10-Q68L are shown in Figure 6, C and D. These images show that although GFP-Rab10-Q68L remains associated with Tf-containing endosomes, a large fraction is strikingly relocalized to a condensed apical compartment lacking internalized Tf. This compartment is distinct from the TGN, as determined by furin immunofluorescence (Figure 6E).

The redistribution of the Q68L mutant is more easily appreciated in Video 2, which shows 3D renderings of image volumes of Tf-labeled cells expressing either the wild-type or Q68L mutant form of GFP-Rab10.

Although the images shown here were collected from fixed cells, identical redistributions of the T23N and Q68L mutant forms of GFP-Rab10 were obtained in studies where image volumes of living cells were collected (our unpublished data).

GTP-Hydrolysis Mutant Q68L-Rab10 Is Associated with the ARE

When the distribution of GFP-Rab10-Q68L was compared with that of basolaterally internalized Tf and IgA, it was found to closely associate with the ARE, as identified as the apical compartment heavily labeled with internalized IgA, but lacking internalized Tf (Figure 7, A and B). The relocalization of Rab10 to the ARE induced by the Q68L mutation in these cells is more obvious in Video 3, which shows 3D renderings of internalized IgA (labeled red) in cells expressing either wild-type or Q68L forms of GFP-Rab10. Note that, whereas much of the GFP-Rab10-Q68L is associated with the ARE, the remainder appears to associate with Tf in common endosomes.

To compare the distribution of Rab10 with the ARE-associated Rab11a, plasmids encoding YFP chimeras of wild-type and Q68L Rab10 were constructed and cotransfected into polarized PTR cells along with plasmids encoding CFP-Rab11a. As shown in Figure 7, C and D, YFP-Rab10 is distributed to distinct vesicles below the level of the CFP-Rab11a–labeled ARE. In contrast, YFP-Rab10-Q68L is almost completely coincident with CFP-Rab11a in the ARE. This comparison is more easily appreciated in Video 4, which shows 3D renderings of image volumes of cells expressing CFP-Rab11a and either the wild-type or Q68L mutant form of YFP-Rab10. The ARE localization of GFP-Rab10-Q68L was also indicated by its codistribution with immunolocalized Rab11a in an apical compartment lacking Tf (our unpublished data).

The effect of the Q68L mutation on the distribution of GFP-Rab10 was quantified, using the image cross-correlation analysis described above. As shown in Figure 7E, the Q68L mutation nearly doubled the correlation of the distribution of Rab10 with IgA in the region of the ARE, increasing the correlation to match that between Rab11a and IgA (Figure 5A). The redistribution of GFP-Rab10 to the ARE induced by the Q68L mutation was also reflected in a more than twofold increase in the correlation between Rab10 and immunolocalized Rab11a. As expected, the redistribution of Rab10 to the ARE induced by the Q68L mutation decreased its correlation with the distribution of internalized Tf by around fourfold.

Expression of Mutant Forms of Rab10 Has No Effect on Membrane Polarity in Polarized MDCK Cells

The common endosomes have been previously associated with the process of sorting of membrane proteins to the basolateral membrane (Odorizzi *et al.*, 1996; Futter *et al.*, 1998; Sheff *et al.*, 1999; Wang *et al.*, 2000), a process mediated by Rab8, the Rab protein most closely related to Rab10 (Ang *et al.*, 2003). This, combined with the redirection of Rab10 to the ARE by the Q68L mutation, suggested that expression of mutant Rab10 may alter endocytic sorting and/or the basolateral polarity of the Tf receptor.

To quantitatively evaluate the effects of expression of the different forms of Rab10 on intracellular sorting of TfR, we conducted a cross-correlation analysis between the projected images of internalized Tf and IgA in cells expressing the different constructs. In a previous study, we found that brefeldin A blocked basolateral sorting of internalized Tf from IgA and that the resulting mis-direction of Tf to the ARE was reflected in an increased correlation between the distribution of internalized IgA and Tf. The results of these studies are summarized in Figure 8. Similar to our previous studies (Wang *et al.*, 2001), treatment of cells with brefeldin A more than tripled the correlation between the distributions of internalized Tf and IgA, reflecting BFA-induced transport of Tf to the IgA-enriched ARE.

No such dramatic effects were observed in cells expressing the various forms of Rab10. Expression of GFP-Rab10-Q68L had no significant effect, and expression of the GFP chimera of the wild-type protein or T23N mutant had small, but statistically significant effects on the correlation, causing a slight increase and a slight decrease, respectively.

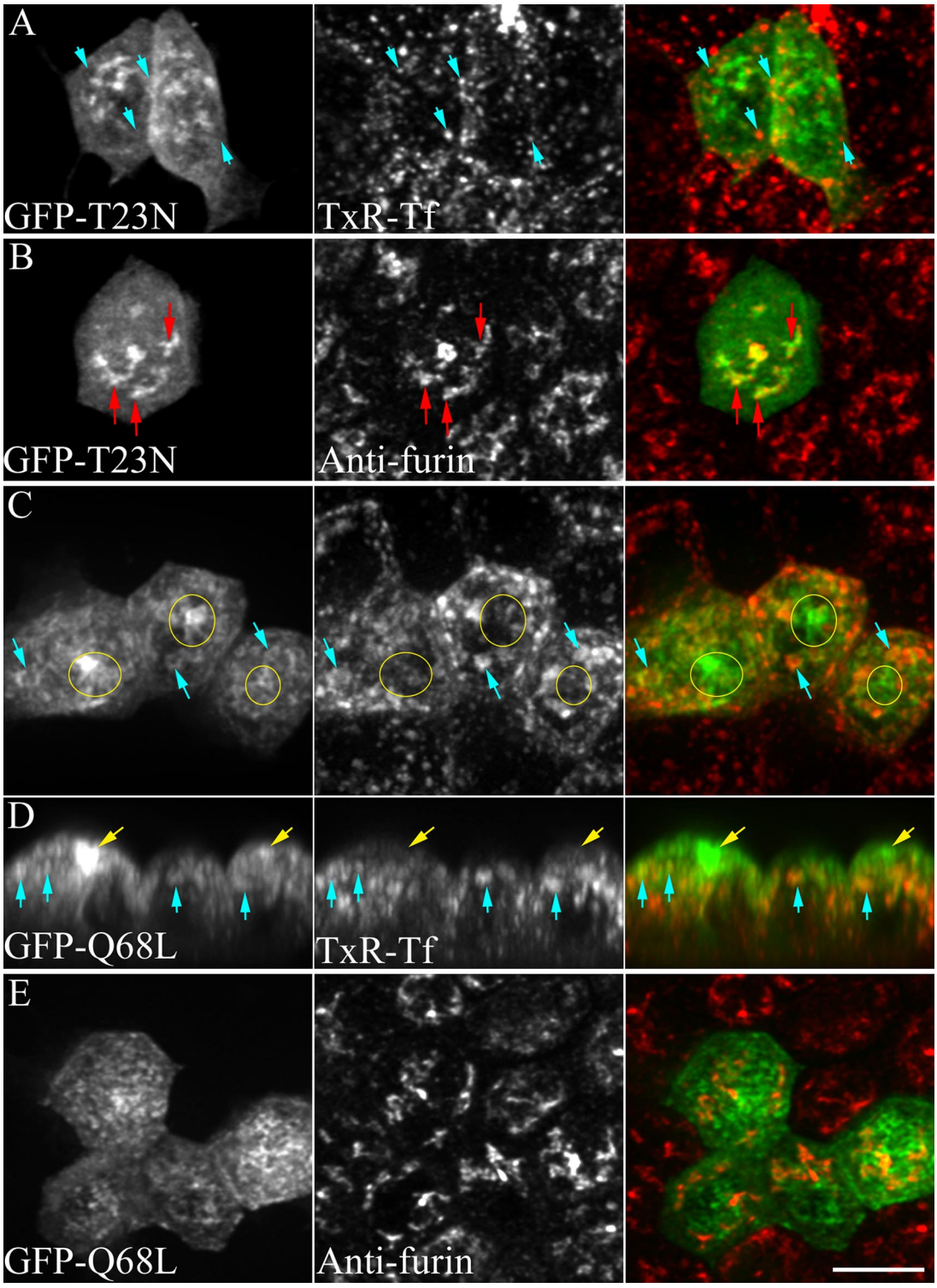

Figure 6. Compartmental localization is altered in GTP-hydrolysis and GTP-binding mutant forms of Rab10. (A) Polarized MDCK cells expressing GFP-Rab10-T23N were incubated for 20 min with TxR-Tf (red) and fixed. Unlike wild-type Rab10, the T23N mutant form of GFP-Rab10 localizes to tubular compartments distinct from Tf-containing endosomes. (B) A projected image volume of a cell expressing GFP-Rab10-T23N and processed for furin immunofluorescence demonstrates that the T23N mutant is relocated to the TGN. (C and D) Polarized MDCK cells expressing GFP-Rab10-Q68L were incubated for 20 min with TxR-Tf and fixed. Although some of the Q68L GFP-Rab10 associates with Tf-containing endosomes (indicated with blue arrows), a large fraction relocates to an apical compartment lacking Tf (indicated with yellow circles in the *XY* projection in C and yellow arrows in the *XZ* projection in D). Volume renderings of the cells shown in C, along with those of Figure 1C, showing cells expressing wild-type GFP-Rab10, are shown in Video 2. (E) Comparison with immunolocalized furin (red) shows that the Q68L mutant form of GFP-Rab10 does not associate with the TGN. Scale bar, 10 μm.

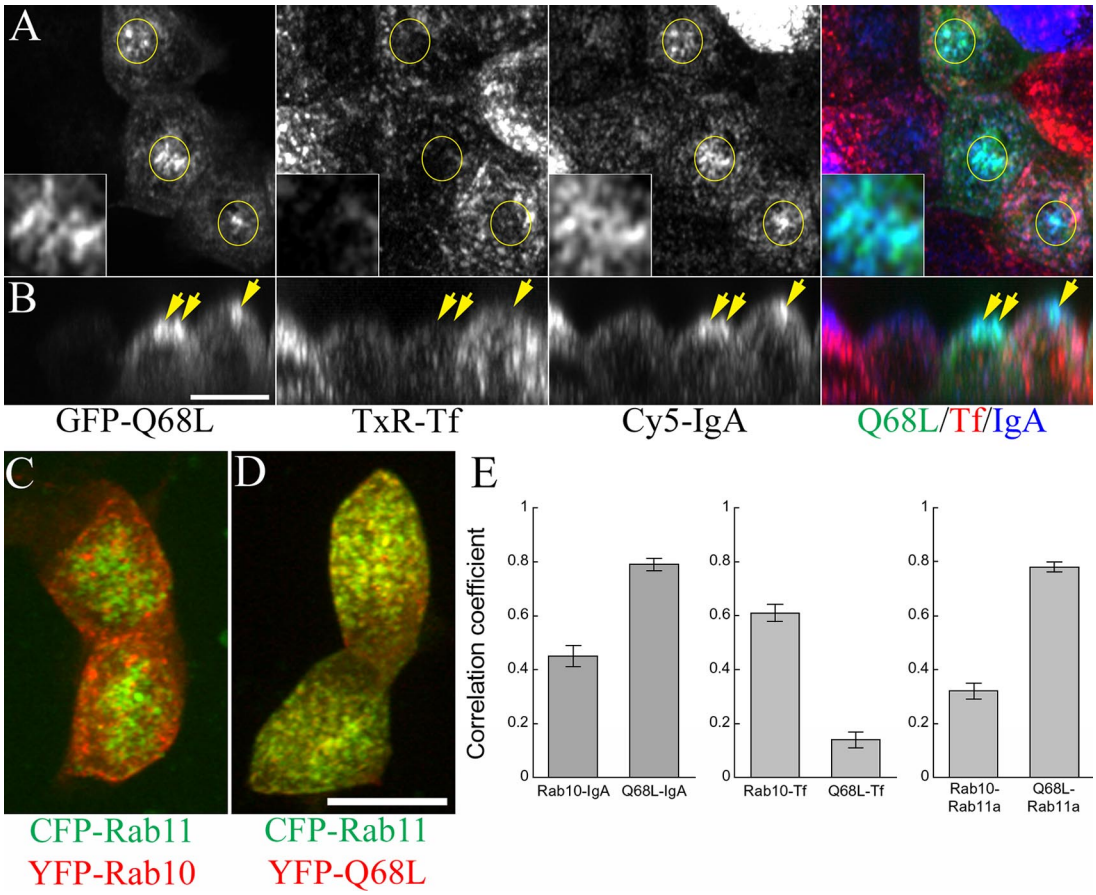

Figure 7. The Q68L mutant form of GFP-Rab10 is redistributed to the ARE of polarized MDCK cells. (A and B) Cells expressing GFP-Rab10 were incubated with TxR-Tf and Cy5-IgA in the basolateral medium for 20 min and fixed. In both *XY* projections (A) and *XZ* projections (B), the Q68L mutant is seen to strongly associate with the ARE, identified as containing internalized IgA, but not Tf. The 2× magnification inset shows the close correspondence between the patterns of GFP-Rab10-Q68L and internalized IgA in the ARE region of one cell. Volume renderings of the cells shown in A, along with those of Figure 4A, showing cells expressing wild-type GFP-Rab10, are shown in Video 3. (C) Image projection of cells coexpressing YFP-Rab10 and CFP-Rab11a. (D) Image projection of cells coexpressing YFP-Rab10-Q68L and CFP-Rab11a. The image volumes of C and D are reproduced as rotating volume renderings in Video 4. Scale bars, 10 μm. (E) The Q68L mutation relocates GFP-Rab10 from common endosomes to the ARE. Left, image cross-correlation analyses comparing the distribution of Cy5-IgA with either GFP-Rab10 or GFP-Rab10-Q68L in the ARE region from projected 3D image volumes collected of transfected cells labeled for 20 min with Cy5-IgA. Middle, the distribution of Cy5-IgA is much more highly correlated with GFP-Rab10-Q68L (r = 0.79, n = 30) than with GFP-Rab10 (r = 0.45, n = 22). The opposite relationship is found for internalized TxR-Tf, which is more highly associated with GFP-Rab10 (r = 0.61, n = 22) than with GFP-Rab10-Q68L (r = 0.14, n = 30). Right, correlation analysis of immunolocalized Rab11a with either GFP-Rab10 or GFP-Rab10-Q68L shows that, as with the comparison with IgA, the Q68L mutation increases the correlation between Rab11a and GFP-Rab10 from 0.32 (n = 20) to 0.78 (n = 20). Differences in all three comparisons were statistically significant, with $p \ll 0.0001$. Data are presented as means ± SEM.

These results suggest that overexpression of GFP chimeras of wild-type and mutant Rab10 has little effect on intracellular sorting of internalized Tf from IgA. To more sensitively evaluate the effect on Tf receptor sorting, we examined the polarity of TfR, as reflected by uptake of Tf from the apical and basolateral sides of the monolayer. In previous work, we found that treatment of cells with brefeldin A increased the expression of Tf receptor at the apical plasma membrane, as reflected in a 10-fold increase in endocytosis of Tf from the apical side of the monolayer (Wang *et al.*, 2001). This result was reproduced in the study shown in Figure 9A, which shows that treatment of cells with brefeldin A results in a significant internalization of Tf from the apical plasma membrane, which is undetectable in control cells. Similar studies of cells expressing wild-type and mutant GFP-Rab10 showed no effects on polarized uptake of Tf; apical uptake of Tf was undetectable in all cases (Figure 9, B–D).

That the expression of GFP chimeras of wild-type and mutant Rab10 had no effect on membrane polarity is also indicated by the observation that the apical polarity of the apical membrane protein GP135 (canine podocalyxin) was, in all cases, unaffected by overexpression of the GFP-Rab10 constructs (Figure 9E).

Expression of Wild-type and Mutant Forms of Rab10 Has No Effect on Basolateral Recycling of Transferrin in Cells Labeled to Steady State

Because both apical and basolateral endocytic pathways traverse common endosomes, proteins associated with common endosomes may regulate the trafficking kinetics of either pathway. To study the effects of expression of wild-type

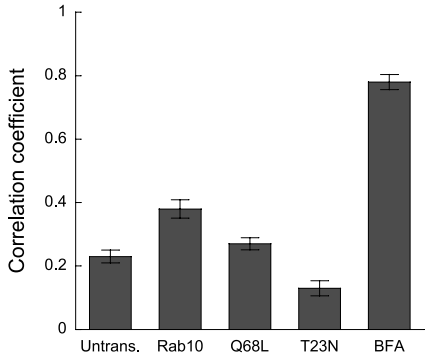

Figure 8. Cross-correlation analysis of sorting of internalized IgA from Tf. Cells were incubated for 20 min with basolateral TxR-Tf and Cy5-IgA and fixed. Three-dimensional image volumes were collected, and correlation analysis was performed comparing the distribution of Cy5-IgA and TxR-Tf from projected 3D image volumes of each cell. Analyses were conducted for untransfected cells (n = 30), cells expressing GFP-Rab10 (n = 20), cells expressing GFP-Rab10-Q68L (n = 30), and cells expressing GFP-Rab10-T23N (n = 16). In each case, only minor effects were observed, although the effects of expression of GFP-Rab10 and GFP-Rab10-T23N were both statistically significant ($p = 0.0001$ and $p < 0.005$, respectively). These effects were dwarfed when compared with those seen in cells treated with 10 μM brefeldin A for 10 min before and during the incubations. This treatment induces misdirection of internalized Tf to the ARE, resulting in more than a threefold increase in the correlation between Tf and IgA (increasing *r* from 0.23 to 0.78). Data are presented as means ± SEM.

and mutant GFP-Rab10 on endocytic kinetics, we developed single-cell fluorescence methods that are independent of transfection efficiency and also allow correlation of effects with levels of protein expression. These methods are described more fully in *Materials and Methods.*

To measure the steady state rate of basolateral recycling, cells were incubated in the presence of TxR-Tf and Cy5-Tf for 25 min and then in Cy5-Tf alone for an additional 10 min. Because 35 min is sufficient to label all Tf receptors on the recycling endocytic pathway (Apodaca *et al.,* 1994; Odorizzi *et al.,* 1996; Brown *et al.,* 2000), the sum of the TxR-Tf and Cy5-Tf fluorescence (after standardization) is proportional to the total number of Tf receptors in the cells. Thus the ratio of the fluorescence of TxR-Tf to the sum of TxR-Tf and Cy5-Tf fluorescence can be used to quantify a specific recycling rate (see details in *Materials and Methods*). Although similar results are obtained if recycling is quantified simply from the mean TxR-Tf fluorescence of the population of cells, the ratiometric quantification has the virtue of standardizing for the number of Tf receptors in the cell. Because the number of Tf receptors varies between cells, this quantification reduces the coefficient of variation in kinetics measurements up to fourfold.

The results of these studies are shown in Figure 10A, which shows that expression of mutant and wild-type GFP-Rab10 had no effect on rates of Tf receptor recycling. Closer analysis showed no correlation between recycling rates and the amount of transfected protein (as measured from total cellular GFP fluorescence), over a 12–30-fold range (our unpublished data). The validity of this assay is demonstrated by the fact that quantitation of these results indicates a half-time of Tf receptor recycling of 7.4 min, very similar to our previous measurement of 8 min using a biochemical assay of ^{125}I-Tf efflux (Brown *et al.,* 2000).

The morphological studies presented in Figures 6, 7, and 9 indicated that expression of mutant forms of Rab10 had no effect on rates of Tf uptake. An approach similar to that described above was taken to evaluate this question quantitatively. For these studies, cells were incubated for 30 min in the presence of Cy3-Tf and then in the presence of both Cy3-Tf and Cy5-Tf for an additional 4 min. As in the recycling assay, the sum of the Cy3-Tf and Cy5-Tf fluorescence (after standardization) is proportional to the total number of Tf receptors in the cells. Internalization is then quantified as the ratio of Cy5-Tf fluorescence divided by the sum of standardized Cy3-Tf and Cy5-Tf fluorescence. Because the rate at which cells acquire Cy5-Tf fluorescence depends not only on the rate of Cy5-Tf internalization, but also on the rate at which receptors reappear at the plasma membrane, this assay is also sensitive to variations in recycling rates. However, because the previous studies showed nearly superimposable recycling kinetics for the different conditions, this assay will report only differences in internalization.

The results of these studies are summarized in Figure 10B, which shows that expression of mutant forms of Rab10 had little effect on the rate of Tf uptake. Expression of GFP-Rab10 caused a small, but statistically significant, 14% decrease in the rate of Tf internalization. The decrease in internalization rate was not related to the amount of cellular GFP-Rab10 over a 25-fold range, as measured from total cellular GFP fluorescence (our unpublished data).

Expression of Mutant Forms of GFP-Rab10 Increases Basolateral Recycling from an Early Compartment

Previous studies have demonstrated that there are two recycling pathways followed by internalized Tf, a slow pathway involving passage through a late compartment and a faster pathway in which Tf recycles directly from an earlier compartment (Presley *et al.,* 1993; Sheff *et al.,* 1999; Hao and Maxfield, 2000). The recycling assay described above will primarily detect differences in recycling from the later compartments, which dominates the efflux kinetics of cells labeled to steady state. To assay the role of Rab10 in recycling from early compartments, the efflux of a brief pulse of fluorescent Tf was measured. In this assay, cells were incubated with TxR-Tf for 20 min at 37°C, rinsed in ice-cold medium 1 for 10 min, incubated with Cy5-Tf for 2 min at 37°C, rinsed in ice-cold medium 1 for 10 min, incubated with TxR-Tf for 4 min at 37°C, and then fixed. Recycling was then quantified from the ratio of Cy5-to-TxR fluorescence in individual cells. Because a significant amount of the Cy5-Tf is still on the internalization pathway during the 4-min chase interval, it is not feasible to measure the "starting" Cy5/TxR ratio before recycling. Thus we have quantified recycling relative to that observed at 22°, a condition under which recycling is slowed (Salzman and Maxfield, 1988; Le *et al.,* 1999; Baravelle *et al.,* 2005). Thus the quantities obtained will provide conservative estimates of recycling, but estimates that are useful for relative comparisons.

As shown in Figure 10C, similar rates of Tf recycling were found in untransfected cells and in cells expressing GFP-Rab10, both of which retained ~70% of the Cy5-Tf retained by cells incubated at 22 μ. However, the rates of recycling were significantly increased in cells expressing GFP-Rab10-Q68L, and especially in cells expressing GFP-Rab10-T23N, which recycled Cy5-Tf at nearly twice the rate of untransfected cells.

These results suggest that expression of mutant forms of Rab10 increases recycling from an early compartment on the basolateral recycling pathway, a compartment we refer to as the "sorting endosome." Although as described above, MDCK cells sort basolaterally internalized Tf from IgA, Sheff *et al.* (1999) demonstrated that recycling via this path-

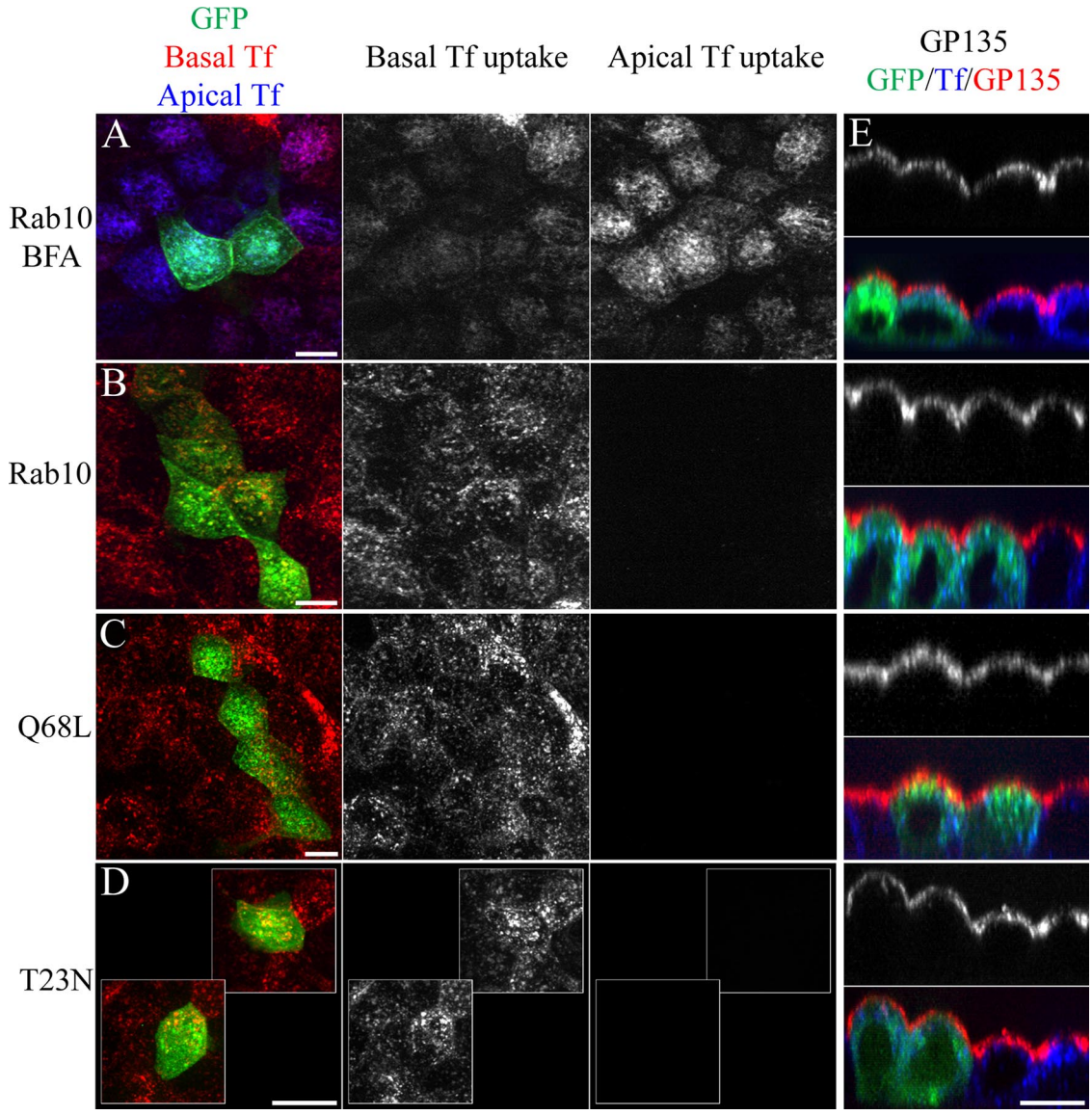

Figure 9. Expression of wild-type and mutant GFP-Rab10 has no effects on basolateral polarity of TfR or on apical polarity of GP135. (A–D) Cells expressing the various forms of GFP-Rab10 (green) were incubated for 25 min with Cy5-Tf (blue) on the apical side and TxR-Tf (red) on the basal side of cell monolayers and fixed. Cells in A were treated with 10 μM brefeldin A for 10 min before and during the incubation. Although brefeldin A treatment results in mistargeting of TfR to the apical membrane, as reflected by significant internalization of Tf from the apical membrane (A), no such effects were seen in cells expressing GFP-Rab10 (B), GFP-Rab10-Q68L (C), or GFP-Rab10-T23N (D). (E) Cells expressing the various forms of GFP-Rab10 (green) were incubated for 20 min with Cy5-Tf (blue), fixed, and processed for GP135 immunofluorescence (red). The apical polarity of GP135 was unaffected by treatment of cells with brefeldin A or by expression of GFP-Rab10, GFP-Rab10-Q68L, or GFP-Rab10-T23N. Scale bars, 10 μm.

way is relatively nonspecific, mediating the rapid basolateral recycling of basolaterally internalized Tf and IgA with nearly equivalent kinetics. Thus, if expression of mutant forms of Rab10 increase recycling from basolateral early (sorting) endosomes, we would expect to see similar effects on the efflux of basolaterally internalized IgA.

Because only a fraction of pIgR recycles, it is not possible to label the complement of recycling pIgR to steady state. Thus a different approach was used to assay IgA efflux in which the IgA content of the same fields of labeled cells was quantified at the beginning and end of a chase period. The assays of basolateral efflux of IgA are complicated by the fact that although Tf is efficiently recycled to the basolateral membrane, basolaterally internalized IgA is effluxed to both apical and basolateral membranes. Insofar as the study of transiently transfected cells requires single-cell analyses, we cannot distinguish these two pathways. However, similar to the assays of recycling of Tf from early endosomes, the relative contribution of the transcytotic pathway can be decreased by limiting the duration of labeling. The brevity of labeling for these studies is limited by the relatively dim fluorescence of IgA in endosomes, which requires longer incubations to generate sufficient signal, especially to quantify signal decreases. Because the half-time of IgA transcytosis is two to four times slower than the half-time of TfR recycling, with half-times of 20–50 min (Futter *et al.*, 1998; Henkel *et al.*, 1998; Leung *et al.*, 1999; Brown *et al.*, 2000), a 20-min incubation was used, a duration sufficient to provide

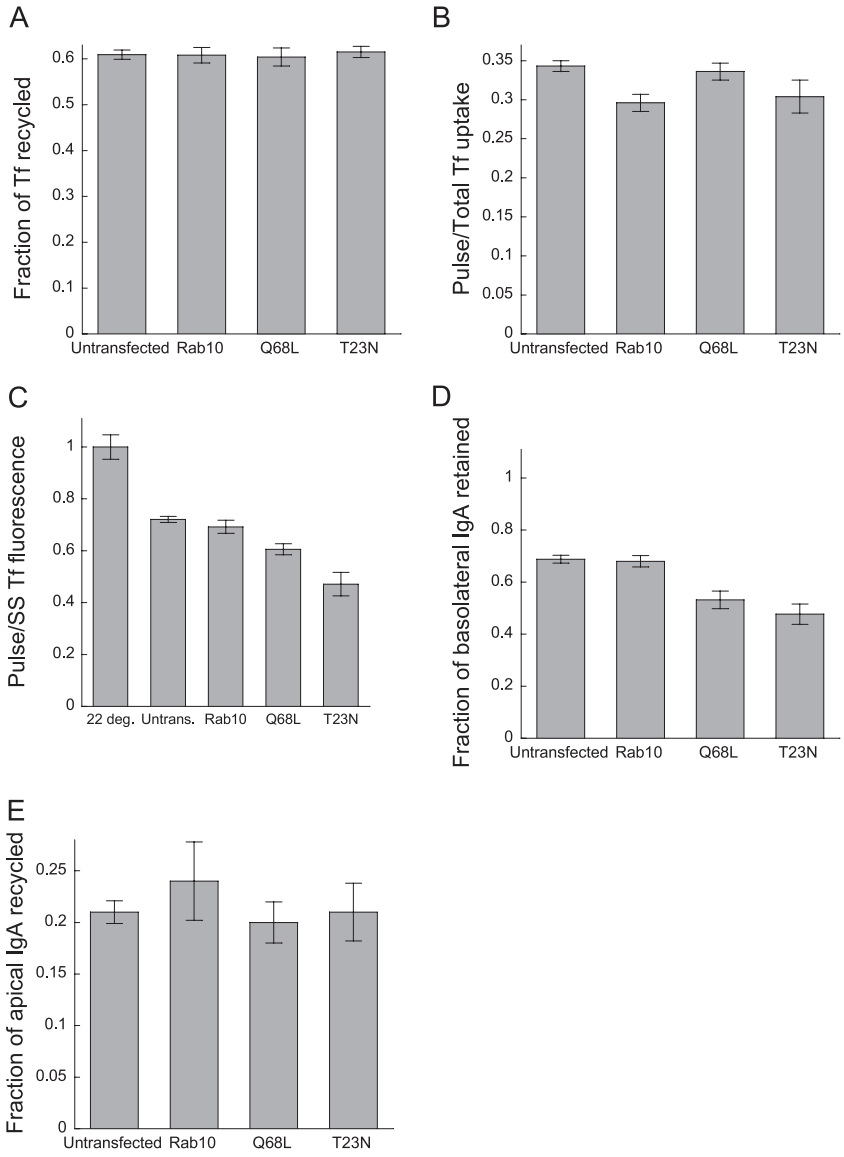

Figure 10. Effects of expression of wild-type and mutant GFP-Rab10 on endocytic traffic in polarized MDCK cells. (A) Effects on recycling of TfR internalized to steady state. Cells expressing different forms of GFP-Rab10 were incubated with basolateral TxR-Tf and Cy5-Tf for 25 min and then in Cy5-Tf alone for an additional 10 min and fixed. The total amount of TxR and Cy5 fluorescence associated with each cell was calculated from the summed image planes and the rate of Tf recycling calculated as described in *Materials and Methods.* Similar rates of recycling were observed in all conditions: 0.61 for untransfected cells ($n = 24$) and cells expressing GFP-Rab10 ($n = 16$, $p = 0.95$), 0.60 for cells expressing GFP-Rab10-Q68L ($n = 22$, $p = 0.85$), and 0.62 for cells expressing GFP-Rab10-T23N ($n = 15$, $p = 0.72$). None of these differences are statistically significant. Data shown are representative of two separate experiments. (B) Effects on basolateral uptake of Tf. Uptake was quantified by incubating cells for 30 min with Cy3-Tf and then with both Cy3-Tf and Cy5-Tf for an additional 4 min. As described in *Materials and Methods,* the rate of Tf uptake was quantified as the fraction of total steady state cell-associated fluorescence resulting from the Cy5-Tf internalized during the pulse period. For untransfected cells, Cy5-Tf internalized for 4 min accounted for 34% of the internalized Tf fluorescence ($n = 66$). No statistically significant effects were induced by expression of either the Q68L (34%, $n = 21$, $p = 0.63$) or T23N mutant (30%, $n = 13$, $p = 0.10$), and a small, but statistically significant decrease in uptake was found in cells expressing GFP-Rab10 (30%, $n = 28$, $p = 0.0006$). (C) Effects on recycling of TfR from early compartments**.** Cells were incubated with TxR-Tf for 20 min at 37°C, rinsed in ice-cold medium 1 for 10 min, incubated with Cy5-Tf for 2 min at 37°C, rinsed in ice-cold medium 1 for 10 min, incubated with TxR-Tf for 4 min at 37°C, and then fixed. Recycling was quantified from the ratio of Cy5-to-TxR fluorescence in individual cells. Recycling rates are standardized relative to that observed at 22°, a condition under which recycling is slowed. No statistically significant differences were found between untransfected cells ($n = 63$) and cells expressing GFP-Rab10 ($p = 0.334$, $n = 29$), but Cy5/TxR ratios were significantly lower in cells expressing either T23N ($p < 0.0001$, $n = 19$) or Q68L ($p < 0.0001$, $n = 20$). Data shown are representative of three different experiments. (D) Effects on cellular efflux of basolaterally internalized IgA**.** Cells were incubated with Cy5-IgA in the basolateral medium for 20 min, washed, and then incubated in the absence of IgA for an additional 20 min, with 100 μg/ml trypsin included in the apical and basolateral media. Image volumes of the same cells were collected at the beginning and end of the chase interval, and recycling was assayed by the fractional decrease in fluorescence. No statistically significant differences were found between untransfected cells ($n = 63$) and cells expressing GFP-Rab10 ($p = 0.76$, $n = 31$), but efflux rates were significantly higher in cells expressing either T23N ($p < 0.0001$, $n = 19$) or Q68L ($p < 0.0002$, $n = 22$). Data shown are representative of two different experiments. (E) Effects on recycling of apically internalized IgA. Cells were incubated with fluorescent IgA in the apical medium for 30 min, washed, and incubated in medium lacking IgA for an additional 12 min, with 100 μg/ml trypsin included in the apical and basolateral media. Image volumes of the same cells were collected at the beginning and end of the chase interval, and recycling was assayed by the fractional decrease in fluorescence. No statistically significant differences were found between untransfected cells ($n = 109$) and cells expressing GFP-Rab10 ($p = 0.31$, $n = 33$), T23N ($p = 0.96$, $n = 28$), or Q68L ($p = 0.51$, $n = 48$). Data shown are pooled from three replicate experiments. Data are presented as means ± SEM.

adequate signal with relatively little IgA in downstream transcytotic compartments. Cells were incubated with fluorescent IgA in the basolateral medium, washed, and then incubated in the absence of IgA for an additional 20 min. Image volumes of the same cells were collected at the beginning and end of the chase interval, and recycling was assayed by the fractional decrease in fluorescence.

The results of these studies, shown in Figure 10D, are very similar to those of the studies of Tf recycling from early endosomes. As in those studies, similar rates of IgA efflux were found in untransfected cells and cells expressing GFP-Rab10, but rates of IgA efflux were significantly increased in cells expressing GFP-Rab10-Q68L, and especially in cells expressing GFP-Rab10-T23N.

Expression of Mutant Forms of GFP-Rab10 Has No Effect on Rates of Apical IgA Recycling

The similar effects of mutant forms of Rab10 on the efflux of basolaterally internalized IgA and on the efflux of Tf from early compartments suggests that the mutants alter basolat-

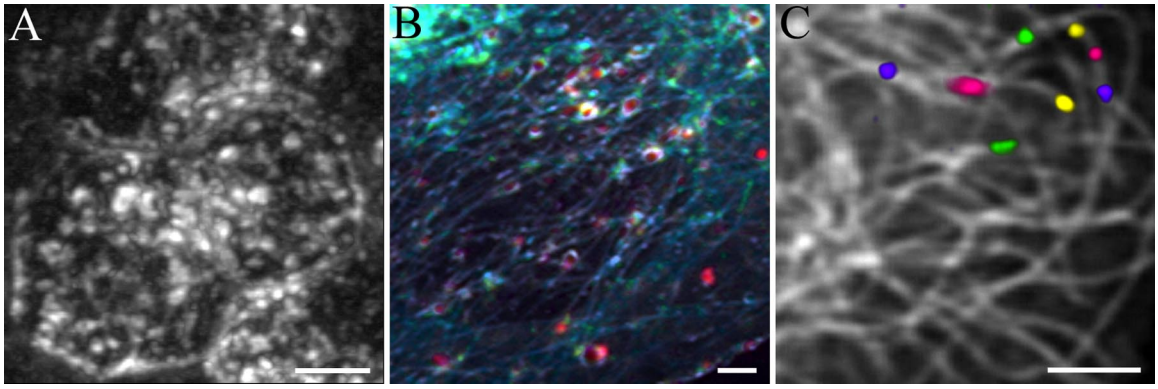

Figure 11. Rab10 associates with highly dynamic transport vesicles that carry Tf between endosomes. (A) Polarized MDCK cells grown on solid permeable supports were transfected with GFP-Rab10 and imaged alive by confocal microscopy. A time series of 3D image volumes were collected at a rate of 0.85 volumes per second, each volume consisting of 26 images spaced 0.6 μm apart. A projection of the first volume is shown in this figure. Video 5a shows the entire time series of projected image volumes, and Video 5b shows the time series displayed as stereo anaglyphs. The movies play at 15 times their actual rate. (B) MDCK cells grown on solid substrates were transfected with GFP-tubulin and GFP-Rab10 and imaged alive in the presence of extracellular TxR-Tf by confocal microscopy. Images were alternately collected of GFP and TxR fluorescence at a rate of 4 pairs per second over a period of 60 s. The image shows the distribution of TxR (red) and GFP (green) for a single time point, with the blue channel showing the average fluorescence of GFP over the entire time series, which has the effect of emphasizing the relatively static microtubules. Fifty seconds of the time series is shown in Video 6, which plays at seven times actual rate. The presence of TxR-Tf in the GFP-Rab10–associated vesicles is demonstrated at the end of the movie, when one portion of the movie is replayed and contrast enhanced to alternately show GFP or TxR in one region of the field. (C) MDCK cells grown on solid substrates were transfected with GFP-tubulin and GFP-Rab10 and imaged alive for 50 s at a rate of five frames per second. The panel shows the summary of a 6-s period, in which the endosomes positions at 15, 16, 19, and 21 s are coded sequentially in purple, red, yellow, and green, respectively. Microtubule labeling is accentuated by showing the mean fluorescence of a 34-frame interval in white. Twenty-nine seconds of this time series is shown in Video 7, which plays at 3.5 times the actual rate. Scale bars, 5 μm in A and 2 μm in B and C.

eral efflux of IgA from basolateral sorting endosomes. However, these studies do not exclude the possibility that expression of the mutants increases efflux of basolaterally internalized IgA from downstream compartments on the transcytotic pathway, such as the common endosomes or apical recycling endosomes. Our previous studies have demonstrated that these later compartments are shared with the apical recycling pathway, as labeled with IgA internalized from the apical plasma membrane (Wang *et al.,* 2000). Thus, if expression of mutant forms of Rab10 increases apical transport of IgA through common endosomes and apical recycling endosomes, we would predict that expression of mutant Rab10 should likewise increase recycling of apically internalized IgA. In contrast, if mutant forms of Rab10 increase basolateral efflux of IgA from basolateral sorting endosomes, which are not included on the apical recycling pathway, they should have no effect on recycling of apically internalized IgA.

For these studies, cells were incubated with fluorescent IgA in the apical medium for 30 min, washed, and incubated in medium lacking IgA for an additional 12 min. Image volumes of the same cells were collected at the beginning and end of the chase interval, and recycling was assayed by the fractional decrease in fluorescence. Trypsin, 100 μg/ml, was included in the apical and basolateral media during the chase, to ensure release of recycled IgA (Apodaca *et al.,* 1994; Brown *et al.,* 2000).

The results of these studies are presented in Figure 10E. Transfection of cells with either wild-type or mutant forms of Rab10 had no significant effect on the rates of efflux of apically internalized IgA. Half-times of recycling varied between 30 min for cells expressing GFP-Rab10 up to 37 min for cells expressing GFP-Rab10-Q68L, but none of the differences were statistically significant. These rates of efflux are similar to, but slightly longer than those previously reported using biochemical methods (~30 min, Henkel *et al.*1998; Leung *et al.,* 1999; Rojas *et al.,* 2001). The fact that expression of mutant forms of Rab10 had no effect on apical recycling is consistent with the hypothesis that expression of the mutants increased efflux of basolaterally internalized IgA from sorting endosomes, rather than increasing the rate of IgA transcytosis.

Rab10 Associates with Highly Dynamic Transport Vesicles That Carry Tf between Endosomes

The results above suggest that Rab10 negatively regulates rapid recycling from basolateral sorting endosomes. One possible mechanism might be that Rab10 mediates transport of Tf and IgA from basolateral sorting endosomes to common endosomes. When this function is inhibited, as by the overexpression of mutant Rab10, Tf and IgA may accumulate in sorting endosomes, increasing their direct efflux to the basolateral plasma membrane. According to this model, Rab10 would be expected to associate with transport vesicles. The yeast homologue of Rab10, Sec4p, is predominantly associated with motile secretory vesicles that mediate transport of newly synthesized proteins to the exocyst, the site of new bud formation (Guo *et al.,* 1999; Schott *et al.,* 2002). The studies presented above demonstrate a close association of Rab10 with common endosomes, but provide little evidence of Rab10 in small transport vesicles. To more sensitively detect vesicular Rab10, high-speed confocal imaging of living cells was conducted.

For these studies, 3D image volumes of polarized MDCK cells expressing GFP-Rab10 were collected at a rate of 22 images per second, so that image volumes were collected nearly at the rate of one per second. These studies demonstrate surprisingly dynamic vesicular traffic of GFP-Rab10. They also demonstrate the importance of viewing transfected cells in time series because the vesicles, which are quite obvious in time series, are so dimly fluorescent that they are difficult to distinguish in static images. Figure 11A

shows a projected image of the first 3D image volume from a time series collected at the rate of 0.85 image volumes (each consisting of 26 image planes) per second over a period of 60 s. The entire time series is shown as a series of projected images in Video 5a or as a series of stereo anaglyphs in Video 5b, each of which plays at 15 times the rate of collection. As in the figures of fixed cells, GFP-Rab10 can be seen bounding relatively large endosomes, but the movies also show GFP-Rab10 on rapidly moving vesicles.

To determine whether these transport vesicles mediate transport of Tf between endosomes, high-speed imaging was conducted on living PTR cells expressing GFP-tubulin and GFP-Rab10, incubating in TxR-Tf. For these studies, cells were grown on coverslips, which results in a more horizontal presentation of the cell that is more conducive to capturing vesicular dynamics by confocal microscopy. Confocal images were collected, alternately collecting GFP or TxR fluorescence at a rate of four pairs per second over a period of 50 s. The resulting movie, which plays at seven times the actual rate, is shown in Video 6, a single frame of which is presented in Figure 11B. As in the figures of fixed cells, GFP-Rab10 can be seen surrounding relatively large, Tf-containing endosomes, but the movie also shows GFP-Rab10 on rapidly moving vesicles, frequently moving along microtubules between endosomes.

At the end of Video 6, the contrast in one subregion is increased to alternately present the TxR-Tf image and the GFP-Rab10 image. As the time series of this inset is toggled forward and backward, one can see that the GFP-Rab10–associated vesicle contains internalized TxR-Tf and that this vesicle is trafficking between two endosomes.

The association of Rab10 transport vesicles with microtubules is more obvious in Figure 11C, which shows a portion of a cell expressing GFP-tubulin and GFP-Rab10. Confocal images of GFP fluorescence were collected at a rate of five frames per second over a 30-s period. In this figure, the tubulin signal was enhanced by averaging a series of 34 sequential frames, and the sequential positions of two vesicles imaged at 15, 16, 19 and 21 s are displayed in purple, red, yellow, and green, respectively. In the resulting time series (Video 7, which plays at 3.5 times the actual rate) numerous vesicles can be observed clearly moving along microtubules.

Although Rab10 is associated with motile vesicles, expression of either mutant form of Rab10 had no observable effect on the dynamics of endosomes, nor on the association of endosomes with microtubules, suggesting that Rab10 function is not necessary for microtubule-based vesicle motility.

DISCUSSION

Rab10 Associates with Common Endosomes, Distinct from the ARE

In contrast to previous studies of fibroblasts (Chen *et al.*, 1993), sea urchin embryonic cells (Leaf and Blum, 1998), and *C. elegans* intestinal epithelia (Chen *et al.*, 2006), the studies presented here demonstrate that Rab10 does not associate with the *trans*-Golgi network of polarized MDCK cells, but rather with endosomes accessible to both the apical and basolateral recycling pathways. Although the number and nature of the compartments on the recycling pathway of MDCK cells is controversial, quantitative morphological analyses demonstrate that Rab10 associates with common endosomes, distinct from the ARE. Our previous studies demonstrated that the ARE can be distinguished from common endosomes by its accumulation of internalized IgA and depletion of internalized Tf (Brown *et al.*, 2000; Wang *et al.*, 2000, 2001). Consistent with this, a correlation analysis demonstrates that the distribution of the ARE marker Rab11a is highly correlated with that of internalized IgA, but negatively correlated with that of internalized Tf. The same analysis of Rab10 shows that the distribution of Rab10 is highly correlated with that of internalized Tf but not with that of internalized IgA, nor with Rab11a. These studies thus identify Rab10 as a marker of common endosomes and also demonstrate that the ARE and common endosomes can be clearly distinguished by their strong associations with Rab11a and Rab10, respectively.

To evaluate the function of Rab10, we have utilized an approach in which we overexpressed GFP chimeras of mutant and wild-type forms of Rab10. Although this approach must be treated cautiously because the behavior of the transfected protein may be altered by overexpression and/or addition of GFP, it has proved useful in the study of numerous Rab proteins, including the closely related Rab8 (Ang *et al.*, 2003), Rab13 (Marzesco *et al.*, 2002), and yeast Sec4p (Schott *et al.*, 2002). Although abnormal behaviors induced by overexpression cannot be excluded, our morphological and kinetic analyses demonstrated that cells expressing a GFP chimera of the wild-type Rab10 behaved very similarly to untransfected cells and that the effects of the different GFP-Rab10 constructs were consistent over a wide range of expression levels and were restricted to a subset of membrane transport pathways. We were unable to immunolocalize endogenous Rab10 with available antibodies, but the appropriate localization of GFP-Rab10 was supported by observations of identical distributions for exogenously expressed HA- or FLAG epitope–tagged Rab10 (our unpublished data).

Rab10 Mediates Transport from Basolateral Sorting Endosomes to Common Endosomes

Analyses of the endocytic kinetics of Tf and IgA demonstrated that expression of mutant forms of Rab10 increased recycling from early compartments. These results contrast with studies of Rab4, a protein associated with recycling from basolateral early endosomes (Sheff *et al.*, 1999) in which expression of a GTP-binding mutant *decreased* the rate of Tf recycling (McCaffrey *et al.*, 2001). Although the inhibition of recycling induced by expression of the mutant Rab4 indicates that Rab4 is necessary for recycling, the enhanced recycling induced by expression of mutant Rab10 suggests that Rab10 somehow negatively regulates recycling from basolateral sorting endosomes. Although this may be true, an alternative model for Rab10 function involves regulation of an alternative efflux pathway from basolateral sorting endosomes. It has been previously demonstrated that there are two efflux pathways from basolateral sorting endosomes, one directly to the basolateral plasma membrane and the other to common endosomes (Sheff *et al.*, 1999). To the degree that Rab10 is necessary for transport from sorting endosomes to common endosomes, expression of mutant forms of Rab10 might be expected to disrupt this transport pathway, thereby increasing the amount of Tf in sorting endosomes and increasing its efflux via the alternative, direct pathway to the basolateral membrane. Thus we suggest that Rab10 may mediate transport from sorting endosomes to common endosomes (Figure 12).

This model is consistent with several observations from this and previous studies. First, we predict that recycling from common endosomes should be unaffected by expression of mutant Rab10. Our data indicate that although transport to common endosomes may be slowed in cells express-

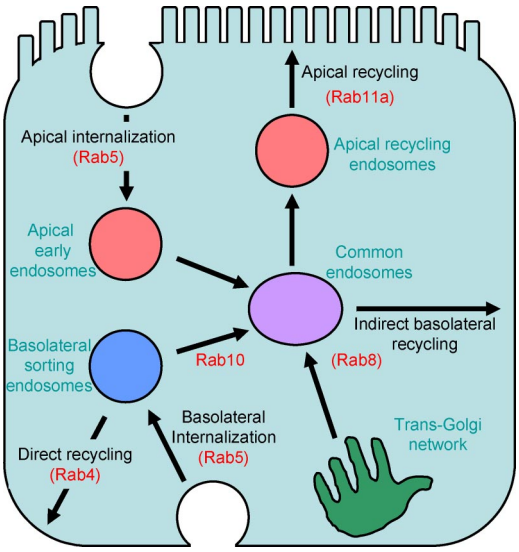

Figure 12. Model of the role of Rab10 in membrane transport in polarized MDCK cells. Endocytic ligands are internalized from both apical and basolateral plasma membrane domains into distinct populations of apical and basolateral early endosomes. Contents from these two pathways are rapidly mixed in a set of common endosomes, which then sort proteins to either the basolateral plasma membrane or to the ARE, from which they are then effluxed to the apical plasma membrane. Rab5 has been shown to regulate endocytic uptake (Gorvel *et al.*, 1991; Bucci *et al.*, 1992) and has been associated with both apical and basolateral early endosomes (Bucci *et al.*, 1994). Proteins mediating transport from apical early endosomes have not yet been described, but the results presented here suggest that Rab10 mediates transport from basolateral sorting endosomes to common endosomes. Transport from the TGN to the basolateral membrane via common endosomes is mediated by Rab8 (Ang *et al.*, 2003). Transport of apically directed contents via the apical recycling endosomes is mediated by Rab11a (Wang *et al.*, 2000a). Although the protein regulators of the direct basolateral recycling pathway have not been identified, Rab4 has been associated with the early compartment that mediates this pathway (Sheff *et al.*, 1999). This diagram is a greatly simplified version of what is known about the molecular regulation of membrane traffic in polarized MDCK cells.

ing mutant Rab10, it is not blocked altogether. Thus even in cells expressing mutant Rab10, the bulk of Tf internalized for an extended period is downstream of sorting endosomes, a distribution that would emphasize efflux from common endosomes. Consistent with our model, we find that expression of mutants has no detectible effect on recycling of Tf from cells labeled to steady state.

Second, Sheff *et al.* (1999) demonstrated that recycling from early basolateral compartments is nonselective, so that both IgA and Tf efflux via this pathway. Thus we expect that expression of mutant forms of Rab10 should likewise increase efflux of basolaterally internalized IgA. Indeed, we found a pattern similar to the effects of the mutants: as in the studies of Tf recycling from early compartments, expression of Rab10-T23N dramatically increased efflux of basolaterally internalized IgA, with cells expressing Rab10-Q68L showing an intermediate effect.

Third, we have previously demonstrated that the apical and basolateral recycling pathways converge at the level of the common endosomes (Figure 12). Thus the apical recycling pathway should be independent of any effects of mutant Rab10 on transport from basolateral sorting endosomes to common endosomes. Consistent with this, we find that expression of mutant forms of Rab10 has no significant effect on the rates of recycling of apically internalized IgA.

Fourth, we find Rab10 associated with common endosomes and to a lesser extent, with sorting endosomes. Studies of living cells demonstrate that Rab10 associates with Tf-containing vesicles trafficking between endosomes, consistent with its suggested role in sorting endosome-to-common endosome transport.

Finally, these studies are highly consistent with results of a recent study of the role of Rab10 in *C. elegans* (Chen *et al.*, 2006), who likewise identify a role for Rab10 in the early basolateral recycling pathway of intestinal epithelia. This study demonstrated that Rab10 is associated with endosomes on the basolateral recycling pathway and that Rab10-null mutants accumulate basolaterally internalized cargo and accumulate swollen Rab5-positive basolateral early endosomes, while losing downstream recycling compartments. As in the studies presented here, these observations are most consistent with a model in which Rab10 mediates transport from basolateral sorting endosomes to common endosomes.

Taken together, these studies strongly indicate that Rab10 mediates transport from basolateral sorting endosomes to common endosomes. A variety of Rab proteins have been characterized in polarized MDCK cells (Rodman and Wandinger-Ness, 2000), but Rab10 is the first of these proteins associated with this transport step.

Alternative Model—the Role of the ARE in Basolateral Membrane Recycling

In our model, we have interpreted that early recycling occurs from sorting endosomes, with the later recycling pathway arising from common endosomes (Figure 12). However, there is some controversy about these designations, specifically about whether the common endosomes are in fact distinct from the ARE and thus whether the slow component of Tf recycling occurs via the ARE (Sheff *et al.*, 1999). In large part, we believe that this controversy reflects differences in how the ARE is defined. Previous studies have identified a condensed, peri-centriolar compartment that accumulates Tf in MDCK cells, referring to this compartment as the "recycling endosome" (Ang *et al.*, 2003). Although we likewise observe an accumulation of Tf in apically localized endosomes, we also detect an additional compartment that is enriched in IgA internalized from either the apical or basolateral plasma membrane, regulated to a higher lumenal pH, and depleted of internalized Tf (Brown *et al.*, 2000; Wang *et al.*, 2000). In addition, the studies described here distinguish this compartment by its association with Rab11a, but not with Rab10, which associates with common endosomes. The low concentration of Tf in the ARE is incompatible with a model of slow recycling from the ARE, which would be expected to result in an accumulation of Tf in the ARE, similar to the accumulation of Tf in the peri-nuclear recycling compartment, which mediates slow recycling in CHO cells (Yamashiro *et al.*, 1984; Presley *et al.*, 1993). Rather, the small amounts of Tf in the ARE are consistent with the rates of apical mis-sorting of TfR (Brown *et al.*, 2000), suggesting that the ARE plays no role in basolateral membrane transport. This conclusion is supported by studies demonstrating that proteins associated with the ARE as identified above (Rab11a, Rab25, Myosin Vb) regulate apical but not basolateral membrane transport (Wang *et al.*, 2000a; Lapierre *et al.*, 2001).

Mechanism of the Inhibitory Effects of Mutant Forms of GFP-Rab10 on the Function of Endogenous Rab10

Early endosome membrane transport was significantly disrupted by overexpression of Rab10-T23N, indicating that this predicted GTP-binding mutant has dominant effects on the function of endogenous Rab10. It is generally believed that GTP-binding mutant forms of GTPases inhibit the function of endogenous GTPases by binding and thereby sequestering GTPase exchange factors (GEFs; Feig, 1999). These "dead-end complexes" competitively inhibit the formation of the GTP-bound, activated form of the endogenous GTPase. This mechanism has been demonstrated to underlie the dominant-negative effects observed by expression of GTP-binding mutant forms of Sec4p (Collins *et al.,* 1997; Walch-Solimena *et al.*, 1997), Ras (Feig and Cooper, 1988; Hwang *et al.,* 1993; Schweighoffer *et al.,* 1993), Rab3a (Burstein *et al.,* 1992), Rab3d (Chen *et al.*, 2003), and Ypt1 (Jones *et al.,* 1995). Thus the dominant effects of Rab10-T23N may reflect competitive binding of the mutant protein to a Rab10 GEF.

Similar, although less pronounced effects on early endosome membrane transport were observed in cells expressing Rab10-Q68L. These observations contrast with those of several other GTPases, such as Ras, Rab5, and Rab7, whose function is augmented by expression of "dominant-active" GTPase hydrolysis mutants, resulting in a phenotype opposite that of cells expressing the "dominant-negative" GTP-binding mutant (Barbacid, 1987; Stenmark *et al.,* 1994; Bucci *et al.,* 2000). However, in this respect Rab10 is similar to the closely related Sec4p, whose function is inhibited by overexpression of either the GTP-binding or GTP-hydrolysis mutants (Walworth *et al.,* 1989, 1992). Thus unlike Ras, the function of Rab10 and Sec4p may not depend upon the level of the GTP-bound form so much as upon a cycle of GTP binding and hydrolysis. According to this model, cycling of the endogenous protein is inhibited by sequestration of a Rab effector protein through high-affinity binding to the GTP-hydrolysis mutant.

Alternatively, Rab10-Q68L may inhibit the function of endogenous Rab10 by mislocalizing Rab10 effectors to the ARE. The function of endogenous Ras can be inhibited by expression of a constitutively active form of Ras lacking membrane association determinants, which is believed to result in sequestration of Ras effectors in the cytosol (Stacey *et al.,* 1991).

Although Rab proteins were once considered as markers of specific transport compartments, it is increasingly appreciated that their distributions are dynamic, determined by cycles of GTP binding and hydrolysis (Ali and Seabra, 2005). In our model, Rab10 cycles between sorting endosomes and common endosomes, with GTP-binding mediating association of Rab10 with the membranes of sorting endosomes and GTP hydrolysis mediating its dissociation from common endosomes. The fact that the bulk of Rab10 localizes to common endosomes suggests that GTP hydrolysis is rate-limiting, leading to an accumulation of Rab10 in the target compartment, common endosomes. The predominant association of Rab10 with the target compartment is similar to Rab5, Rab7, and Rab11a, all of which are largely associated with their transport targets, early endosomes, late endosomes, and recycling endosomes, respectively.

At first glance, the striking relocation of Rab10 carrying the Q68L mutation to the ARE is surprising. However, because Rab10-Q68L is effectively locked in the GTP-bound state and thus locked onto membranes, its distribution may well reflect nonselective bulk membrane transport to compartments downstream of common endosomes, including the ARE, much in the same way that bulk membrane markers are transported to the peri-nuclear recycling compartment of fibroblasts (Mayor *et al.,* 1993; Presley *et al.,* 1993).

We find that although the majority of Rab10-T23N is cytosolic, a fraction is frequently associated with the TGN of polarized MDCK cells. This localization may not be functionally meaningful, because the corresponding mutation disrupts the association of Sec4p (the yeast homologue of Rab10) with Rab-GDI, which is necessary for appropriate membrane targeting (Collins *et al.,* 1997). However, the distribution of Rab10-T23N may suggest that this GDP-locked Rab10 interacts with a TGN-localized GEF. To the degree that these interactions vary between cell types or species, localization to the TGN may predominate in some tissues, perhaps explaining the previous observations of Rab10 in peri-nuclear structures adjacent to and partially overlapping with markers of the Golgi complex and the TGN of fibroblasts (Chen *et al.,* 1993), sea urchin embryonic cells (Leaf and Blum, 1998), and intestinal epithelia of *C. elegans* (Chen *et al.,* 2006). In fact, we occasionally observe Rab10 in the TGN of incompletely polarized cells (our unpublished data), suggesting that its distribution and thus its function may be developmentally regulated.

These results suggest that under certain conditions, Rab10 may play a role in TGN transport. In this regard, it is interesting to note that Rab8, a protein with which Rab10 shares 66% amino acid identity (Chen *et al.,* 1993) likewise associates with recycling endosomes, but regulates basolateral transport of newly synthesized proteins (vesicular stomatitis virus G-protein and LDL receptor), suggesting a role in TGN-to-plasma membrane transport via recycling endosomes. However, in contrast to studies of Rab8, in which expression of the GTP-hydrolysis mutant disrupted the basolateral polarity of the LDL receptor (Ang *et al.,* 2003), expression of mutant forms of Rab10 had no effect on basolateral polarity of TfR nor on apical polarity of gp135.

CONCLUSIONS

Taken together, these observations suggest that Rab10 mediates transport from basolateral sorting endosomes to common endosomes, the first protein associated with this transport step. Rab10 is also the first protein marker of common endosomes and when compared with Rab11 clearly distinguishes common endosomes from the ARE. Because we find little evidence of the wild-type protein in any compartment other than common endosomes, the itinerary of Rab10 would apparently involve transient associations of Rab10 with sorting endosomes. Insofar as the GTP-hydrolysis and GTP-binding mutant forms of Rab10 stabilize interactions between Rab10 and its effectors or GEFS, they may be useful in identifying crucial Rab10-interacting proteins, thus illuminating the molecular regulation of Rab10 and basolateral membrane transport in polarized epithelial cells.

ACKNOWLEDGMENTS

We thank J. Byars, P. Fonarev, P. Schweinsburg, and Barbara Sturonas-Brown for technical assistance. Microscopy studies were conducted at the Indiana Center for Biological Microscopy. This work was supported by National Institutes of Health (NIH) Grant DK51098, a grant (Indiana Genomics Initiative) from the Lilly Endowment to the Indiana University School of Medicine (K.D.), NIH Grant GM67237, MOD Grant 5-FY02, and support from the Chicago Community Trust Searle Scholars Program (B.G). C.C. was supported by the Anne B. and James B. Leathem Scholarship Fund.

REFERENCES

Ali, B., and Seabra, M. (2005). Targeting of Rab GTPases to cellular membranes. Biochem. Soc. Trans. *33*, 652–656.

Ang, A., Folsch, H., Koivisto, U.-M., Pypaert, M., and Mellman, I. (2003). The Rab8 GTPase selectively regulates AP-1b-dependent basolateral transport in polarized Madin-Darby canine kidney cells. J. Cell Biol. *163*, 339–350.

Apodaca, G., Katz, L., and Mostov, K. (1994). Receptor-mediated transcytosis of IgA in MDCK cells is via apical recycling endosomes. J. Cell Biol. *125*, 67–86.

Baravelle, G., Schober, D., Huber, M., Bayer, N., Murphy, R., and Fuchs, R. (2005). Transferrin recycling and dextran transport to lysosomes is differentially affected by bafilomycin, nocodazole and low temperature. Cell Tissue Res. *320*, 99–113.

Barbacid, M. (1987). Ras genes. Annu. Rev. Biochem. *56*, 779–827.

Breitfeld, P., Casanova, J., Harris, J., Simister, N., and Mostov, K. (1989). Expression and analysis of the polymeric Ig receptor in Madin-Darby canine kidney cells using retroviral vectors. Methods Cell Biol. *32*, 329–337.

Brown, P., Wang, E., Aroeti, B., Chapin, S., Mostov, K., and Dunn, K. (2000). Definition of distinct compartments in polarized MDCK cells for membrane-volume sorting, polarized sorting and apical recycling. Traffic *1*, 124–140.

Bucci, C., Mather, I., Stunnenberg, H., Simons, K., Hoflack, B., and Zerial, M. (1992). The small GTPase rab5 functions as a regulatory factor in the early endocytic pathway. Cell *70*, 715–728.

Bucci, C., Wandinger-Ness, A., Lutcke, A., Chiriello, M., Bruni, C., and Zerial, M. (1994). Rab5a is a common component of the apical and basolateral endocytic machinery in polarized epithelial cells. Proc. Natl. Acad. Sci. USA *91*, 5061–5065.

Bucci, C., Thomsen, P., Nicoziani, P. McCarthy, J., and van Deurs, B. (2000). Rab7, a key to lysosome biogenesis. Mol. Biol. Cell *11*, 467–480.

Burstein, E., Brondyk, W., and Macara, I. (1992). Amino acid residues in the ras-like GTPase Rab3a that specify sensitivity to factors that regulate the GTP/GDP cycling of Rab3a. J. Biol. Chem. *267*, 22715–22718.

Casanova, J., Wang, X., Kumar, R., Bhartur, S., Navarre, J., Woodrum, J., Altschuler, Y., Ray, G., and Goldenring, J. (1999). Association of Rab25 and Rab11a with the apical recycling system of polarized Madin-Darby canine kidney cells. Mol. Biol. Cell *10*, 47–61.

Chavrier, P., Vingron, M., Sander, C., Simon, K., and Zerial, M. (1990). Molecular cloning of YPT1/SEC4-related cDNAs from an epithelial cell line. Mol. Cell. Biol. *10*, 6578–6585.

Clendenon, J., Phillips, C., Sandoval, R., Fang, S., and Dunn, K. (2002). Voxx, a PC-based near real-time volume rendering system for biological microscopy. Am. J. Phys. Cell. *282*, C213–C218.

Chen, Y.-T., Holcomb, C., and Moore, H.-P. (1993). Expression and localization of two low molecular weight GTP-binding proteins, Rab8 and Rab10, by epitope tag. Proc. Natl. Acad. Sci. USA *90*, 6508–6512.

Chen, C., Schweinsberg, P., Vashist, S., Mareiniss, D., Lambie, E., and Grant, B. (2006). Rab-10 is required for endocytic recycling in the *C. elegans* intestine. Mol. Biol. Cell (*in press*).

Chen, X., Ernst, S., and Williams, J. (2003). Dominant negative Rab3D mutants reduce GTP-bound endogenous Rab3D in pancreatic acini. J. Biol. Chem. *278*, 50053–50060.

Collins, R., Brennwald, P., Garrett, M., Lauring, A., and Novick, P. (1997). Interactions of nucleotide release factor Dss4p with Sec4p in the post-Golgi secretory pathway of yeast. J. Biol. Chem. *272*, 18281–18289.

Deneka, M., Neeft, M., and van der Sluijs, P. (2003). Regulation of membrane transport by rab GTPases. Crit. Rev. Biochem. Mol. Biol. *38*, 121–142.

Dunn, K., McGraw, T., and Maxfield, F. (1989). Iterative fractionation of recycling receptors from lysosomally destined ligands in an early sorting endosome. J. Cell Biol. *109*, 3303–3314.

Dunn, K., and Maxfield, F. (1992). Delivery of ligands from sorting endosomes to late endosomes occurs by maturation of sorting endosomes. J. Cell Biol. *117*, 301–310.

Feig, L. (1999). Tools of the trade: use of dominant-inhibitory mutants of Ras-family GTPases. Nat. Cell Biol. *1*, E25–E27.

Feig, L., and Cooper, G. (1988). Inhibition of NIH 3T3 cell proliferation by a mutant ras protein with preferential affinity for GDP. Mol. Biol. Cell *8*, 3235–3243.

Feng, Y., Press, B., and Wandinger-Ness, A. (1995). Rab7, and important regulator of late endocytic membrane traffic. J. Cell Biol. *131*, 1435–1452.

Frech, M., Darden, T., Pedersen, L., Foley, C., Charifson, P., Anderson, M., and Wittinghofer, A. (1994). Role of glutamine-61 in the hydrolysis of GTP by p21-H-ras. An experimental and theoretical study. Biochemistry *33*, 3237–3244.

Futter, C., Gibson, A., Allchin, E., Maxwell, S., Ruddock, L., Odorizzi, G., Domingo, D., Trowbridge, I., and Hopkins, C. (1998). In polarized MDCK cells basolateral vesicles arise from clathrin-gamma adaptin-coated domains on endosomal tubules. J. Cell Biol. *141*, 611–624.

Gorvel, J., Chavrier, P., Zerial, M., and Gruenberg, J. (1991). Rab5 controls early endosome fusion in vitro. Cell *64*, 915–925.

Guo, W., Roth, D., Walch-Solimena, C., and Novick, P. (1999). The exocyst is an effector for Sec4p, targeting secretory vesicles to sites of exocytosis. EMBO J. *18*, 1071–1080.

Hao, M., and Maxfield, F. (2000). Characterization of rapid membrane internalization and recycling. J. Biol. Chem. *275*, 15279–15286.

Henkel, J., Apodaca, G., Altschuler, Y., Hardy, S., and Weisz, O. (1998). Selective perturbation of apical membrane traffic by expression of influenza M2, an acid-activated ion channel, in polarized Madin-Darby canine kidney cells. Mol. Biol. Cell *9*, 2477–2490.

Hoekstra, D., Tyteca, D., and van Ijzendoorn, S.C.D. (2004). The subapical compartment: a traffic center in membrane polarity development. J. Cell Sci. *117*, 2183–2192.

Huber, L., Pimplikar, S., Parton, R., Virta, H., Zerial, M., and Simons, K. (1993). Rab8, a small GTPase involved in vesicular traffic between the TGN and the basolateral plasma membrane. J. Cell Biol. *123*, 35–45.

Hwang, Y.-W., Zhong, J.-M., Poullet, P., and A. Parmeggiani. (1993). Inhibition of SDC25 C-domain-induced guanine-nucleotide exchange by guanine ring binding domain mutants of v-H-ras. J. Biol. Chem. *268*, 24692–24698.

Jones, S., Litt, R., Richardson, C., and Segev, N. (1995). Requirement of nucleotide exchange factor for Ypt1 GTPase mediated protein transport. J. Cell Biol. *130*, 1051–1061.

Jununtula, J., DeMaziere, A., Peden, A., Ervin, K., Advani, R., van Dijk, S., Klumperman, J., and Scheller, R. (2004). Rab14 is involved in membrane trafficking between the Golgi complex and endosomes. Mol. Biol. Cell *15*, 2218–2229.

Kohler, K., Louvard, D., and Zahraoui, A. (2004). Rab13 regulates PKA signalling during tight junction assembly. J. Cell Biol. *165*, 175–180.

Lapierre, L., Kuman, R., Hales, C., Navarre, J., Bhartur, S., Burnette, J., Provance, D., Mercer, J., Bahler, M., and Goldenring, J. (2001). Myosin Vb is associated with plasma membrane recycling systems. Mol. Biol. Cell *12*, 1843–1857.

Lau, A., and Mruk, D. (2003). Rab8b GTPase and junction dynamics in the testis. Endocrinology *144*, 1549–1563.

Le, T., Yap, A., and Stow, J. (1999). Recycling of E-cadherin: a potential mechanism for regulating cadherin dynamics. J. Cell Biol. *146*, 219–232.

Leaf, D., and Blum, L. (1998). Analysis of rab10 localization in sea urchin embryonic cells by three-dimensional reconstruction. Exp. Cell Res. *243*, 39–49.

Leung, S., Rojas, R. Maples, C., Flynn, C. Ruiz, W., Jou, T., and Apodaca, G. (1999). Modulation of endocytic traffic in polarized MDCK cells by the small GTPase RhoA. Mol. Biol. Cell *10*, 4369–4384.

Leung, S., Ruiz, W., and Apodaca, G. (2000). Sorting of membrane and fluid at the apical pole of polarized Madin-Darby canine kidney cells. Mol. Biol. Cell *11*, 2131–2150.

Marzesco, A., Dunia, I., Pandjaitan, R., Recouvreur, M., Dauzonne, D., Benedetti, E., Louvard, D., and Zahraoui, A. (2002). The small GTPase Rab13 regulates assembly of functional tight junctions in epithelial cells. Mol. Biol. Cell *13*, 1819–1831.

Mayor, S., Presley, J., and Maxfield, F. (1993). Sorting of membrane components from endosomes and subsequent recycling to the cell surface occurs by a bulk flow process. J. Cell Biol. *121*, 1257–1269.

McCaffrey, M., Bielli, A., Cantalupo, G., Mora, S., Roberti, V., Santillo, M., Drummond, F., and Bucci, C. (2001). Rab4 affects both recycling and degradative endosomal trafficking. FEBS Lett. *495*, 21–30.

Morimoto, S., Nishimura, N., Terai, T., Manabe, S., Yamamoto, Y., Shinahara, W., Miyake, H., Tashiro, S., Shimada, M., and Sasaki, T. (2005). Rab13 mediates the continuous endocytic recycling of occludin to the cell surface. J. Biol. Chem. *280*, 2220–2228.

Moritz, O., Tam, B., Hurd, L., Peranen, J., Deretic, D., and Papermaster, D. (2001). Mutant Rab8 impairs docking and fusion of rhodopsin-bearing post-Golgi membranes and causes cell death of transgenic *Xenopus* rods. Mol. Biol. Cell *12*, 2341–2351.

Odorizzi, G., Pearse, A., Domingo, D., Trowbridge, I. and Hopkins. C. (1996) Apical and basolateral endosomes of MDCK cells are interconnected and contain a polarized sorting mechanism. J. Cell Biol. *135*, 139–152.

Peranen, J., Auvinen, P., Virta, H., Wepf, R., and Simons, K. (1996). Rab8 promotes polarized membrane transport through reorganization of actin and microtubules in fibroblasts. J. Cell Biol. *135*, 153–167.

Pereira-Leal, J., and Seabra, M. (2001). Evolution of the Rab family of small GTP-binding proteins. J. Mol. Biol. *313*, 889–901.

Presley, J., Mayor, S., Dunn, K., Johnson, L., McGraw, T., and Maxfield, F. (1993). The End2 mutation in CHO cells slows the exit of transferrin receptors from the recycling compartment but bulk membrane trafficking is unaffected. J. Cell Biol. *122*, 1231–1241.

Rodman, J., and Wandinger-Ness, A. (2000). Rab GTPases coordinate endocytosis. J. Cell Sci. *113*, 183–192.

Rojas, R., Ruiz, W., Leung, S.-M., Jou, T-S., and Apodaca, G. (2001). Cdc42-dependent modulation of tight junctions and membrane protein traffic in polarized Madin-Darby canine kidney cells. Mol. Biol. Cell *12*, 2257–2274.

Salminen, A., and Novick, P. (1987). A Ras-like protein is required for a post-Golgi event in yeast secretion. Cell *49*, 527–538.

Salzman, N., and Maxfield, F. (1988). Intracellular fusion of sequentially formed endocytic compartments. J. Cell Biol. *106*, 1083–1091.

Schott, D., Collins, R., and Bretscher, A. (2002). Secretory vesicle transport velocity in living cells depends on the myosin-V lever arm length. J. Cell Biol. *156*, 35–39.

Schweighoffer, F., Cai, H., Chevallier-Multon, M., Fath, I., Cooper, G., and Tocque, B. (1993). The *Saccharomyces cerevisiae* SDC25 C-domain gene product overcomes the dominant inhibitory activity of Ha-Ras Asn-17. Mol. Cell. Biol. *13*, 39–43.

Sheff, D., Daro, E., Hull, M., and Mellman, I. (1999). The receptor recycling pathway contains two distinct populations of early endosomes with different sorting functions. J. Cell Biol. *145*, 123–139.

Stacey, D., Feig, L., and Gibbs, J. (1991). Dominant inhibitory Ras mutants selectively inhibit the activity of either cellular or oncogenic Ras. Mol. Cell. Biol. *11*, 4053–4064.

Stenmark, H., Parton, R., Steele-Mortimer, O., Lutcke, A., Gruenberg, J., and Zerial, M. (1994). Inhibition of Rab5 GTPase activity stimulates membrane fusion in endocytosis. EMBO J. *13*, 1287–1296.

Ullrich, O., Reinsch, S., Urbe, S., Zerial, M., and Parton, R. (1996). Rab11 regulates recycling through the pericentriolar recycling endosome. J. Cell Biol. *135*, 913–924.

Walch-Solimena, C., Collins, R., and Novick, P. (1997). Sec2p mediates nucleotide exchange on Sec4p and is involved in polarized delivery of post-Golgi vesicles. J. Cell Biol. *137*, 1495–1509.

Walworth, N., Brennwald, P., Kabcenell, A., Garrett, M., and Novick, P. (1992). Hydrolysis of GTP by Sec4 protein plays an important role in vesicular transport and is stimulated by a GTPase-activating protein in *Saccharomyces cerevisiae*. Mol. Cell. Biol. *12*, 2017–2028.

Walworth, N., Goud, B., Kabcenell, A., and Novick, P. (1989). Mutational analysis of SEC4 suggests a cyclical mechanism for the regulation of vesicular traffic. EMBO J. *8*, 1685–1693.

Wang, E., Brown, P., Aroeti, B., Chapin, S., Mostov, K., and Dunn, K. (2000). Apical and basolateral endocytic pathways of MDCK cells converge in acidic common endosomes distinct from a nearly-neutral apical recycling endosome. Traffic *1*, 480–493.

Wang, X., Kumar, R., Navarre, J., Casanova, J., and Goldenring, J. (2000a). Regulation of vesicle trafficking in Madin-Darby canine kidney cells by Rab11a and Rab25. J. Biol. Chem. *37*, 29138–29146.

Wang, E., Pennington, J., Goldenring, J., Hunziker, W., and Dunn, K. (2001). Brefeldin A rapidly disrupts plasma membrane polarity by blocking polar sorting in common endosomes of MDCK cells. J. Cell Sci. *114*, 3309–3321.

Yamashiro, D., Tycko, B., Fluss, S., and Maxfield, F. (1984). Segregation of transferrin to a mildly acidic (pH 6.5) para-Golgi compartment in the recycling pathway. Cell *37*, 789–800.

Zacchi, P., Stenmark, H., Parton, R., Orioli, D., Lim, F., Giner, A., Mellman, I., Zerial, M., and Murphy, C. (1994). Rab17 regulates membrane trafficking through apical recycling endosomes in polarized epithelial cells. J. Cell Biol. *140*, 1039–1053.

Zahraoui, A., Joberty, G., Arpin, M., Fontaine, J. Hellio, R., Tavitian, A., and Louvard, D. (1994). A small GTPase is distributed in cytoplasmic vesicles in non-polarized cells but colocalizes with the tight junction marker ZO-1 in polarized epithelial cells. J. Cell Biol. *124*, 101–115.

Zuk, P., and Elferink, L. (1999). Rab15 mediates an early endocytic event in Chinese hamster ovary cells. J. Biol. Chem. *274*, 22303–22312.

Zuk, P., and Elferink, L. (2000). Rab15 differentially regulates early endocytic trafficking. J. Biol. Chem. *275*, 26754–26764.